180/
4-28-77

ANL-76-98

ANL-76-98

Dr 958

HIGH-PERFORMANCE BATTERIES FOR OFF-PEAK ENERGY STORAGE AND ELECTRIC-VEHICLE PROPULSION

Progress Report for the Period July–September 1976

MASTER

U of C-AUA-USERDA

ARGONNE NATIONAL LABORATORY, ARGONNE, ILLINOIS

Prepared for the U. S. ENERGY RESEARCH AND DEVELOPMENT ADMINISTRATION under Contract W-31-109-Eng-38

DISTRIBUTION OF THIS DOCUMENT IS UNLIMITED

DISCLAIMER

This report was prepared as an account of work sponsored by an agency of the United States Government. Neither the United States Government nor any agency Thereof, nor any of their employees, makes any warranty, express or implied, or assumes any legal liability or responsibility for the accuracy, completeness, or usefulness of any information, apparatus, product, or process disclosed, or represents that its use would not infringe privately owned rights. Reference herein to any specific commercial product, process, or service by trade name, trademark, manufacturer, or otherwise does not necessarily constitute or imply its endorsement, recommendation, or favoring by the United States Government or any agency thereof. The views and opinions of authors expressed herein do not necessarily state or reflect those of the United States Government or any agency thereof.

DISCLAIMER

Portions of this document may be illegible in electronic image products. Images are produced from the best available original document.

The facilities of Argonne National Laboratory are owned by the United States Government. Under the terms of a contract (W-31-109-Eng-38) between the U. S. Energy Research and Development Administration, Argonne Universities Association and The University of Chicago, the University employs the staff and operates the Laboratory in accordance with policies and programs formulated, approved and reviewed by the Association.

MEMBERS OF ARGONNE UNIVERSITIES ASSOCIATION

The University of Arizona
Carnegie-Mellon University
Case Western Reserve University
The University of Chicago
University of Cincinnati
Illinois Institute of Technology
University of Illinois
Indiana University
Iowa State University
The University of Iowa
Kansas State University
The University of Kansas
Loyola University
Marquette University
Michigan State University
The University of Michigan
University of Minnesota
University of Missouri
Northwestern University
University of Notre Dame
The Ohio State University
Ohio University
The Pennsylvania State University
Purdue University
Saint Louis University
Southern Illinois University
The University of Texas at Austin
Washington University
Wayne State University
The University of Wisconsin

NOTICE

This report was prepared as an account of work sponsored by the United States Government. Neither the United States nor the United States Energy Research and Development Administration, nor any of their employees, nor any of their contractors, subcontractors, or their employees, makes any warranty, express or implied, or assumes any legal liability or responsibility for the accuracy, completeness or usefulness of any information, apparatus, product or process disclosed, or represents that its use would not infringe privately-owned rights. Mention of commercial products, their manufacturers, or their suppliers in this publication does not imply or connote approval or disapproval of the product by Argonne National Laboratory or the U. S. Energy Research and Development Administration.

Printed in the United States of America
Available from
National Technical Information Service
U. S. Department of Commerce
5285 Port Royal Road
Springfield, Virginia 22161
Price: Printed Copy $4.50; Microfiche $3.00

Distribution Category:
Energy Storage—Electrochemical
(UC-94c)

ANL-76-98

ARGONNE NATIONAL LABORATORY
9700 South Cass Avenue
Argonne, Illinois 60439

HIGH-PERFORMANCE BATTERIES FOR OFF-PEAK ENERGY STORAGE AND ELECTRIC-VEHICLE PROPULSION

Progress Report for the Period
July—September 1976

NOTICE
This report was prepared as an account of work sponsored by the United States Government. Neither the United States nor the United States Energy Research and Development Administration, nor any of their employees, nor any of their contractors, subcontractors, or their employees, makes any warranty, express or implied, or assumes any legal liability or responsibility for the accuracy, completeness or usefulness of any information, apparatus, product or process disclosed, or represents that its use would not infringe privately owned rights.

P. A. Nelson — Director, Energy Storage
N. P. Yao — Associate Director, Energy Storage
A. A. Chilenskas — Manager, Battery Commercialization
E. C. Gay — Section Manager, Battery Engineering
R. K. Steunenberg — Section Manager, Advanced Electrochemical Technology
J. E. Battles — Group Leader, Materials Development
F. Hornstra — Group Leader, Battery Charging Systems
W. E. Miller — Group Leader, Industrial Cell and Battery Testing
M. F. Roche — Group Leader, Cell Chemistry
H. Shimotake — Group Leader, Cell Development and Engineering
W. J. Walsh — Group Leader, Advanced Engineering

December 1976

MASTER

Previous Reports in this Series

ANL-75-36	January—June 1975
ANL-76-9	July—December 1975
ANL-76 35	January—March 1976
ANL-76-81	April—June 1976

DISTRIBUTION OF THIS DOCUMENT IS UNLIMITED

PREFACE

Argonne National Laboratory's program on high-temperature secondary batteries is carried out principally in the Chemical Engineering Division, with assistance on specific problems being given by the Materials Science Division and, from time to time, by other Argonne divisions. The individual efforts of many scientists and technicians are essential to the success of the program, and recognition of these efforts is reflected in the individual contributions cited throughout the report.

TABLE OF CONTENTS

		Page
ABSTRACT		1
SUMMARY		2
I.	INTRODUCTION	7
II.	COMMERCIAL DEVELOPMENT	10
	A. Commercialization Plan	10
	B. Systems Design	11
	C. Industrial Contracts	11
	1. Cell Fabrication	11
	2. Electrode Separators	13
	3. Feedthrough Development	14
	4. Computer Program	14
III.	BATTERY ENGINEERING	15
	A. Industrial Cell and Battery Testing	15
	1. Testing of Contractor-Produced Cells	15
	2. Automation of Qualification Testing	17
	3. Battery Testing	18
	4. Cell Testing Facilities	23
	B. Battery Charging Systems	23
	1. Electronic Development	23
	2. Battery Charging Systems for Electric Vehicles	23
	3. Automatic Repair of a Battery Cell with an Open Circuit	25
	C. Cell Development and Engineering	26
	1. Cell Performance and Lifetime Improvement	26
	2. Large-Scale Cell	30
	3. Electrode Development	30
IV.	TECHNOLOGY DEVELOPMENT	33
	A. Materials Development	33
	1. Electrical Feedthrough Development	33
	2. Ceramic Materials Development	34
	3. Electrode Separator Development	37
	4. Corrosion Studies	37
	5. Postoperative Examinations	39

TABLE OF CONTENTS (contd)

	Page
B. Advanced Cell Engineering	41
1. Multiplate Cell Development	42
2. Advanced Electrode Development	44
3. Lifetime Studies	45
C. Cell Chemistry	46
1. Metallographic Study of FeS Electrodes	46
2. Wick and Pool Electrodes for Use in Prismatic and Cylindrical Cells	46
3. Lithium-Silicon Electrodes	48
D. Alternative Secondary Cells	51
1. Preliminary Tests of New Systems	51
2. Negative Electrodes of the Second Kind	52
3. Engineering Cell Tests	53
V. Li-Si/FeS CELL AND BATTERY DEVELOPMENT-- ATOMICS INTERNATIONAL	54
REFERENCES	55
APPENDIX. SUMMARY OF LARGE-SCALE CELL TESTS	56

LIST OF FIGURES

No.	Title	Page
III-1.	Specific Power of Cell EP-2B4 at 430°C.	16
III-2.	Specific Power of Cell EP-2B4 at 400°C.	16
III-3.	Cycle Life History of Cell EP-2B4	17
III-4.	Specific Power of Cell EP-2A5	18
III-5.	Specific Energy *vs.* Discharge Time for Batteries B7-S, B8-P, and B8-S.	20
III-6.	Specific Power of Battery B7-S.	21
III-7.	Specific Power of Battery B8-9.	22
III-8.	Charging and Cell Equalizing System for an Electric-Vehicle Battery.	24
III-9.	Capacity *vs.* Cycle Life for Cell R-15	27
III-10.	Capacity *vs.* Cycle Life for Cells KK-4 and KK-5	27
III-11.	Voltage *vs.* Capacity for Cells KK-5 and KK-6.	28
III-12.	Capacity *vs.* Cycle Life for Cell CB-1	29
III-13.	Voltage *vs.* Capacity for Cell CB-1 at C/5 Rate.	29
III-14.	Voltage *vs.* Capacity for Cell SS-1 at 25 mA/cm^2	31
IV-1.	Foamed Y_2O_3 Separators.	35
IV-2.	Microstructure of the Cell Walls of a Y_2O_3 Foam	36
IV-3.	Y_2O_3 Fibers Prepared by Extrusion	36
IV-4.	Charge-Discharge Curve for Cell A-1	43
IV-5.	Capacity *vs.* Cycle Life for Cell A-1.	44
IV-6.	Structure of Positive Electrodes of Li/LiCl-KCl/FeS Cells During Charging	47
IV-7.	Decline in Li-Si Plateaus with Cycling Owing to Reaction of Silicon with Housing and Current Collector	49
IV-8.	Performance of Li/TiS_2 Cell at 420°C.	52

LIST OF TABLES

No.	Title	Page
I-1.	Performance Goals for Lithium-Aluminum/Metal Sulfide Batteries.	7
III-1.	Summary of Battery Performance at Various Charge and Discharge Rates.	19
IV-1.	Percent of Total Corrosion Occurring at Three Intervals of Cell Discharge.	38
IV-2.	Results of Postoperative Examinations of Four ANL Prismatic Cells.	39
IV-3.	Voltages of Plateaus in the Li-Si System	50

HIGH-PERFORMANCE BATTERIES FOR OFF-PEAK ENERGY STORAGE AND ELECTRIC-VEHICLE PROPULSION

Progress Report for the Period
July-September 1976

ABSTRACT

This report describes the research and management efforts of the program at Argonne National Laboratory (ANL) on lithium-aluminum/metal sulfide batteries during the period July-September 1976. These batteries are being developed for electric-vehicle propulsion and for stationary energy storage applications. The present cells, which operate at 400-450°C, are vertically oriented, prismatic cells with a central positive electrode of FeS or FeS_2, two facing negative electrodes of lithium-aluminum alloy, and an electrolyte of molten LiCl-KCl.

A major goal of the program is to assist in the development of a competitive, self-sustaining industry for the production of Li-Al/metal sulfide batteries. To this end, a market study and an economic analysis are being performed; cells, cell components, and battery testing equipment are being developed and fabricated by industrial firms under contracts with ANL; and work is in progress on designs for a 30 kW-hr electric-vehicle battery and a module for a stationary energy storage battery.

Testing and evaluation of industrially fabricated cells is continuing. During this period, cells fabricated by Eagle-Picher Industries, Inc. were tested as single cells and as two- and three-cell batteries. Design modifications based on evaluations of these tests are in progress. New electrode and cell designs are also being developed and tested at ANL, and promising designs will be incorporated in the industrially fabricated cells. The concepts receiving major attention include the design of multiple-electrode cells, the fabrication of electrodes in the uncharged state (positive electrodes of Li_2S and Fe and negative electrodes of porous aluminum), the use of carbon-bonded current-collector structures in the positive electrode, the fabrication of electrodes by hot-pressing active materials and electrolyte, and the use of additives to the negative electrode to improve electrode performance and extend cell lifetime.

Materials development efforts included optimization of designs of electrical feedthroughs; development of improved electrode separators, *e.g.*, BN and Y_2O_3 felts; corrosion tests of construction materials; and postoperative examination of cells. Cell chemistry studies included the development of a new type of liquid-lithium electrode, in which lithium from a pool is wicked to the positive electrode. Investigations of alternative cell systems included tests of small-scale Li/TiS_2 and $NaFeS_2$ cells; a larger-scale $CaMg_2/FeS$ cell is also being operated.

SUMMARY

Commercial Development

A plan is being formulated to define the elements of commercialization effort whereby a competitive, self-sustaining industry for the production of lithium/metal sulfide batteries can be developed. A market study and an economic analysis have been initiated to identify high-performance battery needs in military, aerospace and industrial applications for the near term (1978-1985). A systems design effort is under way to design a 30 kW-hr electric-vehicle battery; present emphasis is on the design of a compatible cell prototype. The design of a truckable battery module (about 5 MW-hr capacity) for stationary energy storage is also being pursued.

Industrial Contracts. Included as an integral part of the commercialization plan for Li-Al/metal sulfide batteries are contractual arrangements with industrial firms to develop and fabricate cells, cell components, battery components, and battery testing equipment. Industrial contractors are continuing to supply a variety of 12.7 x 12.7 cm Li-Al/FeS_2 cells for testing. Design variations include an improved connection between the molybdenum terminal and the positive electrode current collector, cells with Y_2O_3 felt electrode separators, Li-Al electrodes of 55 at. % Li, and FeS_2 cells assembled in the uncharged state. Performance of a test cell fabricated in air was sufficiently promising to justify further development of this technique.

The development of cell components to meet technical and cost goals is being pursued by a number of industrial contractors. Electrode separators being evaluated include BN bonded paper, composites of BN, asbestos, and MgO powder; and Y_2O_3 felts. A ram-type electrical feedthrough is being redesigned in an effort to reduce its size. Work is under way to develop cold-pressed yttria parts and a nonmetallic braze for feedthrough production.

An industrial participant contract was recently started to provide a computer program for load-profile simulations for electric vehicle batteries. A load-profile program has been put into an ANL computer, and modifications peculiar to our application are in progress.

Industrial Cell and Battery Testing

Cell Tests. First-generation Li-Al/FeS_2 cells fabricated by Eagle-Picher Industries, Inc. are presently being tested at ANL. The electrodes in these cells were made by cold-pressing the active powders into honeycomb current collector structures. The FeS_2 cells are of two types; they differ from each other principally in electrode thickness. For the Type B cells, the negative electrode thicknesses are 0.7 cm and the positive electrode half-thicknesses are 0.6 cm. For Type A cells, the corresponding dimensions are all 0.35 cm.

Cell EP-2B4, a thick cell, has been operated for more than 1750 hr and 130 deep discharge cycles (most of these cycles were at the 6-hr rate for both discharge and charge). Its maximum specific energy was about 80 W-hr/kg; for most of the cycles the value was 60 W-hr/kg. Testing now in progress has shown that the specific energy can be increased, without appreciably altering

the cycle life, by employing a higher charge cutoff voltage. The peak specific energy is now about 87 W-hr/kg and a specific energy of about 70 W-hr/kg is being attained for most cycles. The peak specific power for this type of cell is about 50 W/kg.

Type A thin cells have shown higher specific power but lower specific energy than the Type B cells. For Cell EP-2A5, the peak specific energy is 65 W-hr/kg (at the 5-hr rate) and peak specific power is 67 W/kg. After about 1000 hr of operation, the performance of this thin FeS_2 cell has declined only about 7%.

One result of the tests to date is that the next cells being manufactured by Eagle-Picher will have a higher ratio of active material to total cell weight. This will be done primarily by replacing electrolyte with active materials. This change is expected to increase the specific energy of the cells appreciably.

Battery Tests. Testing of a battery composed of two FeS-type thick cells has continued for more than 90 cycles and 2000 hr, with a specific energy of 62 W-hr/kg at a 10-hr rate and 43 W-hr/kg at a 5-hr rate. Start-up and conditioning of cells in a parallel arrangement has been successfully demonstrated. Performance of cells conditioned in this manner compares favorably with the performance of single cells. Two FeS_2-type thin cells have been tested for a total of 135 cycles and 1560 hr in parallel and in series connections. In the parallel arrangement, the peak specific energy was 59 W-hr/kg at a 5-hr rate, and 43 W-hr/kg was achieved at a 2-hr rate. The peak specific power was 67 W/kg at $\sim$220 A.

Battery Charging Systems

The six-cell monitor/charge controller has been assembled and debugging is in process. The prototype cell equalization systems have been received from Gulton, Inc. Tests show that differential cell charging and excellent charge cutoff voltage regulation are exhibited. The initial charging currents are somewhat less than expected from the design specifications; however, the basic concept appears valid. It is expected that a full scale equalizer based upon the above design for weekend use on an electric vehicle can be mass produced for one dollar per cell. A future program for electric vehicle charging systems is presented. A brief investigation was conducted on the possible use of copper oxide cutouts to automatically bypass an open cell in a battery. The conclusion was that further study and development of various materials for use at the temperature of interest would be needed before the scheme could be applied successfully to high-temperature batteries.

Cell Development and Engineering

Cell Performance and Lifetime Improvement. A series of tests is under way to evaluate uncharged cells with hot-pressed FeS_2 electrodes. The first cell, Cell R-15, is being operated at the 5-hr rate. Studies of three cells with carbon-bonded positive electrodes, Cells KK-4, -5 and -6, are continuing. Although the capacity of Cell KK-4 has declined considerably after operation for 4600 hr and 280 cycles, Cell KK-5 is maintaining its initial performance after 3100 hr and 170 cycles. Cast Li-Al alloy plaques used as negative electrode in Cell KK-5 required a prolonged conditioning period. Cell CB-1, a

charged cell with a carbon-bonded $CuFeS_2$ electrode has accumulated 5350 hr and 365 cycles of operation while maintaining its initial capacity. The depth of discharge in this cell is limited to a low level (~45%); its long life and high performance suggest that a relationship exists between capacity retention and depth of discharge.

Evaluation of New Cell Designs. A multiplate cell having two positive and four negative electrodes, Cell MP-2, continues to operate, after 163 cycles and 1925 hr. It was found that the cell performance was limited by the least efficient of the six electrodes contained in the cell. An improved start-up procedure is being considered. A large-scale cell (24 by 35 cm, 600 W-hr) designed for utility energy storage was recently put into operation. This cell (SS-1) was assembled in the charged state and has a carbon-bonded FeS-Cu_2S positive electrode and two negative electrodes of Li-Al in iron Retimet. The cell has achieved an energy output of 577 W-hr at the 10-hr rate, and has been in operation 40 cycles and 750 hr.

Electrode Development. Three different types of Li-Al negative electrode structures were tested in 12.5 by 12.5 cm prismatic cells. These cells were operated to evaluate the effects on cell lifetime of improved current collection, addition of indium to Li-Al alloy (one of several additives to be tested), and excess Li-Al in the negative electrodes. In Cell R-18, an uncharged Li-Al/FeS cell, the negative electrode was a woven aluminum fabric containing copper-coated steel strands to improve current collection. In Cell FM-1, a charged Li-Al/FeS cell, a small amount of indium was added to the Li-Al electrode, and in Cell EC-1, an uncharged Li-Al/FeS + CoS_2 cell, cast plaques of 25 at. % Li-Al alloy were used as the negative electrode, thereby proving a 50% excess of lithium in the cell. Most of these tests are being continued to assess the effects of these improvements on retention of cell capacity with cycling. The performance of a Li-Si alloy negative electrode was also tested. Cell R-19, a charged Li_4Si/FeS + Cu_2S cell is showing stable performance in start-up cycling at relatively low current densities.

Materials Development

A study was conducted to optimize the parameters for sealing Conax-type compression feedthroughs. The feedthroughs presently in use incorporate a 3/16-in. (0.48-cm) conductor rod, an alumina upper insulator, a compressed boron nitride powder layer, and a boron nitride lower insulator. The measured leak rate in air for these feedthroughs is about 10^{-5} $Pa \cdot m^3/s$. Improvement in design is being sought by the substitution of stronger ceramics such as Y_2O_3 or BeO for the BN lower insulator, which is relatively weak; with Y_2O_3 and BeO, a greater sealing torque can be applied and the leak rates are an order of magnitude smaller for both 0.48 and 0.64-cm conductor rods. Solder glasses are being evaluated as secondary sealants outside the primary boron nitride powder seal to further reduce the leak rate.

Boron nitride and Y_2O_3 felts which had successfully completed 1000-hr in-cell tests as electrode separators were examined with a scanning electron microscope. No evidence of corrosive attack was observed. Yttria felt is presently being used as a separator in a test cell with no particle retainer other than a layer of 325-mesh screen over each electrode face. The cell has been in operation for more than 600 hr, at this writing, with excellent electrical performance and no signs of deterioration.

Separator concepts which do not employ conventional ceramic fiber processing are also being investigated. Effort has been concentrated on the development of open-cell foams and on extruded ceramic fibers. Planned-interval tests of 5000-hr duration have been completed on BeO and Y_2O_3 ceramics. The tests demonstrated the acceptable compatibility of both materials to the cell environment for extended periods of time.

Static corrosion tests were conducted on a group of alloys at 450°C in the positive electrode environments of partially discharged FeS_2 cells; the states of discharge used in the tests were 25, 50, and 75%. Estimates of actual in-cell performance based on the corrosion results indicate that approximately 80% of the total corrosive attack on nickel-base alloys (Hastelloys B and C and Inconels 617 and 625) would occur in the interval from 0 to 25% discharge. For Type 304 stainless steel, about 95% of the total corrosion would be expected in this same interval.

Postoperative examinations were conducted on four vertical prismatic cells fabricated at ANL. In one cell containing an FeS_2 positive electrode with a nickel current collector, the nickel had undergone severe attack. In a similar cell a positive-electrode current collector of Hastelloy B, a molybdenum-rich nickel alloy, showed less evidence of attack and the presence of an adherent MoS_2 layer. In cells with FeS and Cu_2S as positive electrode materials, metallic copper had precipitated within the separator and may have caused short circuits. A separator of yttria felt had been used in one of these cells, and had been compressed to one-quarter of its original thickness by the expansion of the electrodes. The extent of compression, which was much greater than that for BN fabric separators, probably contributed to the shorting problem. An engineering cell of prismatic design fabricated by an industrial firm was examined to determine the effect of operation in air. Only minimal oxidation of the outer cell housing had occurred, and no evidence of internal oxidation was found.

Advanced Cell Engineering

The relative merits of various designs of advanced Li-Al/FeS_x cells are continually being evaluated. Increased emphasis is being placed on the development of FeS_2 cells that operate on the upper voltage plateau ($FeS_2 \rightleftarrows FeS$) because this type of cell appears to have a number of advantages. The primary effort in the Advanced Cell Engineering Group is concentrated in the following areas: (a) mechanisms of lifetime limitation, (b) alternative binary and ternary lithium alloys for use as negative electrodes, (c) large multiple-electrode, upper-plateau cells for load-leveling application and (d) high-performance FeS_2 three-electrode cells for electric vehicle application.

A multiplate cell with several new design features was operated during this period. Cell A-1, an uncharged FeS_2 cell with five electrodes (2 positive and 3 negative), achieved 130 W-hr/kg and operated through 31 cycles and 1075 hr. The cell was designed to minimize interior structural components, improve assembly procedure, and minimize interelectrode spacing. The positive electrode had a one-piece molybdenum current collector which also served as the voltage and current lead. No apparent problems were encountered with electrode mismatching.

Several cells were operated to test the effect of various metal additives to the Li-Al negative electrode. In Cell DK-33, the Li-Al contained 3.9 wt % indium, and the cell had a capacity of 10.27 A-hr. The lithium utilization was excellent. After a decline of only 5% in the first 100 cycles, the utilization remained constant until termination (136 cycles), at which time utilization was 92% at the C/12 rate. In Cell DK-37, 10 wt % lead was added to the Li-Al electrode, which had a theoretical capacity of 7.78 A-hr. No apparent improvement over a cell without the lead additive was noted. The test was terminated after 120 cycles, at which time the lithium utilization was 74% at the C/8 rate and the C/4 rate. Cell DK-39, with 4.9 wt % tin in the negative electrode, is currently in operation. Preliminary data at the C/12 rate indicate a lithium utilization of 95%.

Cell Chemistry

The phases present in an FeS electrode at various stages from full discharge to overcharge have been identified; these phases are illustrated in photomicrographs. A study of wick-and-pool lithium electrodes for use in prismatic and cylindrical cells has been initiated. The concept employs a low-surface-area wick that remains flooded with lithium and a separate storage vessel for the main lithium supply. The feasibility of the electrode concept was demonstrated in a small Li/LiCl-KCl/Al cell.

In studies of Li-Si/Li cells, irreversible loss of silicon was traced to formation of silicides with the current collector and electrode housing. Compounds identified in the Li-Si system agreed well with results of earlier studies at Atomics International, and the compounds were found to be stable to at least 580°C. Plateau emfs were determined over the temperature range 375 to 500°C.

Alternative Secondary Cells

Tests of Li/LiCl-KCl/TiS_2 and Na/LiCl-NaCl-KCl/FeS_2 cells are reported. The TiS_2 positive electrode gave 100% utilization (forming $LiTiS_2$) at current densities as high as 100 mA/cm^2. The phases found in the positive electrode of the Na/FeS_2 cell were the same as in Li/FeS_2 cells because of the presence of LiCl in the electrolyte.

Negative electrodes of the second kind, which consisted of mixtures of LiAl or LiMg and Li_2O, were investigated by slow-sweep cyclic voltammetry. For the LiAl-Li_2O mixture, discharge peaks corresponding to at least two Faradays per mole of aluminum were found in the range -300 to +300 mV *vs.* LiAl, and about four Faradays were obtained over a wide anodic range (-300 to +900 mV *vs.* LiAl). With the LiMg-Li_2O mixture, a two-electron peak at -200 mV *vs.* LiAl and a one-electron peak at +350 mV *vs.* LiAl were observed.

A $CaMg_2$/LiF-LiCl-KCl-$CaCl_2$/FeS cell of 60 A-hr capacity was recently put into operation. After three cycles the coulombic efficiency is ∿100% and calcium utilization is 60% at 10 mA/cm^2 and 28% at 25 mA/cm^2. The performance is expected to improve with cycling.

I. INTRODUCTION

Lithium-aluminum/metal sulfide batteries are being developed at Argonne National laboratory (ANL) for use as (1) power sources for electric vehicles and (2) stationary energy storage devices for load-leveling on electric utilities, and storage of electric energy produced by solar, wind, and other energy sources. Our performance goals for electric vehicle batteries and stationary energy storage batteries are given in Table I-1. These goals have been changed from those given in the preceding report (ANL-76-81) in that short-term goals have been added and long-term goals have been adjusted to reflect new approaches in the battery development effort. Beginning in FY 1977 a clear-cut distinction will be made at ANL in the design characteristics of cells for electric vehicle and stationary energy storage applications. The reason for this distinction is the striking difference in the requirements for the two types of cells, as illustrated in Table I-1.

Table I-1. Performance Goals for Lithium-Aluminum/Metal Sulfide Batteries

	Electric Vehicle Propulsion		Stationary Energy Storage	
Battery Goals	Mark I 1978	Prototype 1985	BEST 1981	Prototype 1985
Power				
Peak	30 kW	60 kW	1.5 MW	25 MW
Sustained Discharge	12 kW	25 kW	1 MW	10 MW
Energy Output	30 kW-hr	45 kW-hr	5 MW-hr	100 MW-hr
Specific Energy,[a] W-hr/kg	110	180	60-80[b]	60-150[b]
Discharge Time, hr	4	4	5	5-10
Charge Time, hr	8	5-8	8	10
Cycle Life	300	1000	1000	3000
Cost of Cells, $/kW-hr	-	35	25-30[c]	20

[a] Includes cell weight only; insulation and supporting structure is approximately 25% of total weight for the Mark I electric vehicle battery and 15 to 20% for the 1985 prototype vehicle battery.

[b] The broader range of values, in comparison with past specific-energy goals, resulted from a reassessment of this requirement (see text).

[c] Projected cost at a production rate of 2000 MW-hr/yr.

The cycle life requirements differ markedly. The cycle life requirement for the Mark I electric vehicle battery is about 300 cycles, which is only a small extrapolation from the actual cycle life of experimental cells. (A life of 400 cycles has already been achieved, but with a loss of capacity that is greater than acceptable.) Even the long-term goal for the electric vehicle battery is only 1000 full cycles. In contrast, initial cells for stationary

energy storage application that will be tested in the Battery Energy Storage Test (BEST) Facility must achieve about 1000 cycles, and the eventual goal is 3000 cycles. To achieve long cell life, compactness will be sacrificed to provide a higher volume fraction of electrolyte and lower swelling pressures, and to allow a more liberal use of retainer materials, and thicker current collectors and cell walls.

The specific energy and specific power goals for electric vehicle cells are much greater than those for stationary energy storage cells, especially for the near-term projects. To achieve the goals for high specific energy and high specific power in electric vehicle cells, we are concentrating our efforts in the near term on developing FeS_2-type cells with one positive and two negative electrodes; these cells are fabricated in the uncharged condition. During charge, FeS_2 is formed in the positive electrode, and the cells are designed for operation on the upper voltage plateau only.

The range of values cited in Table I-1 for the specific energy of the prototype stationary energy storage cells is much broader than we have proposed in the past. Past goals for specific energy of stationary energy storage batteries have been closely linked to the cost goals; hence, our estimates of the required specific energy were made on the basis of projected cost. We now believe that it may be possible to achieve a lower cost for the stationary energy storage battery by developing cells of moderate specific energy that utilize low-cost materials, rather than cells of very high specific energy and lower weight. Therefore, the specific-energy goal for the batteries to be developed for the BEST Facility has tentatively been set at 60-80 W-hr/kg--the low end of the range for the long-term development program.

For the stationary energy storage application, efforts are being concentrated on the development of FeS-type cells, which do not require expensive materials such as molybdenum in the positive electrode. The use of inexpensive separator materials such as pressed composites of powder and fiber is also being emphasized. For the longer term, partial replacement of lithium by less expensive materials such as calcium, sodium, or magnesium will be considered.

Both the near-term and long-term cost goals for the stationary energy storage battery are more stringent than those for the electric vehicle battery. Before a battery can be tested in the BEST Facility, it will be necessary to demonstrate that the cells could be produced at a moderately low cost of about $25-30/kW-hr. Eventually, however, the cost for a stationary energy storage battery cell should be no more than about $20/kW-hr. On the other hand, costs for fabricating the Mark I electric vehicle battery are not an overriding consideration, and projected costs for commercial production are not presently needed.

The differences in near-term goals for the two types of batteries may be summarized as follows. The goals for the Mark I electric-vehicle battery were set for small cells of moderate cycle life, high specific energy, and high specific power, without cost restrictions. In contrast, the goals for the batteries to be installed in the BEST Facility are long cycle life, moderate specific energy and power, and low cost at moderate production rates.

In the long term, the technical goals must be achieved with a battery that can be mass produced commercially at the indicated costs. To accomplish this, contracts have been made with industrial firms to develop and fabricate electrodes and cells, as well as electrode separators, feedthroughs, and battery components. The contractual efforts and the work at ANL on cell design and fabrication, materials development, and battery design are coordinated so that information exchange is rapid and efficient. Cell chemistry studies and advanced cell engineering studies at ANL also provide support for the commercial development effort. A small portion of the overall effort is directed toward investigating promising alternative systems for secondary battery applications.

II. COMMERCIAL DEVELOPMENT
(A. A. Chilenskas)

A. Commercialization Plan

The objective of the commercialization effort is the establishment of a competitive, self-sustaining industry capable of producing a supply of lithium/metal sulfide batteries that meets national needs. This objective is to be accomplished through normal market forces, with a minimum of governmental support. A commercialization plan is under development that will define the essential elements, *i.e.*, the market, product, and need (driving force for change). An essential part of this plan, the market study, has just been initiated; ANL is leading the study and assistance is being given by several industrial participants. The study will be a combination of a market survey and an economic analysis. The market survey will identify high-performance battery needs in military, aerospace and industrial applications for the near term (1978-1985) and will include existing and unfilled needs. Pricing information from the market survey will permit a demand-function (cost-*vs.*-quantity sold) relationship to be established. The economic analysis will permit a projection of (1) the required production of lithium/iron sulfide batteries to satisfy the market for each year and (2) the capital expenditure requirements to support these production rates. In this way, the near-term markets will be used to build an industrial manufacturing base with a minimum of federal support.

The industrial base thus established will be capable of expansion to fulfill the goal of the program, namely, the establishment of a competitive, self-sustaining industry. The commercialization plan will tie together three main elements: technical goals, economics, and environmental/safety considerations. Technical goals for the lithium/metal sulfide batteries have been updated from time to time to reflect the current state of development and projections for the future. In addition, goals have been set with consideration of end-use requirements of the two major applications, that is, utility energy storage and electric vehicle propulsion. In establishing end-use goals, consideration is also given to economic requirements, since the achievement of high performance has an important impact upon the system costs calculated in terms of, for example, dollars/kilowatt-hour of energy storage.

Under the category of economics, an analysis of the technical and economic characteristics of competing systems for major markets will also be undertaken. This analysis is important in determining the cost and pricing policies to be established in the near-term markets. Projected battery costs for both the near-term and long-term markets will be undertaken. Since the battery costs are very sensitive to production scale, costs will be estimated on the basis of the expected yearly markets developed by the market surveys.

Environmental and safety considerations play an important role in the introduction of a new technology into the noninstitutional marketplace. Existing literature already projects a favorable environmental impact (*e.g.*, in air quality) for the use of batteries in vehicles and utility energy storage plants. Consideration needs to be given--and will be given--to the

environmental impact resulting from mining and manufacturing operations related to production of batteries in the near and long term.

The safety requirements for the application of these batteries in the near and long term are to be determined. Some preliminary safety tests, as well as a considerable body of experience in laboratory and industrial fabrication and testing, strongly suggest that the lithium-aluminum/iron sulfide system will be safe to manufacture and use. The recent manufacture and testing of industrially fabricated cells in an air environment, with no adverse effects, further supports this premise.

The market study, which is currently under way, is being directed by the Energy and Environmental Systems Division* of ANL, with assistance from market-oriented members of two commercial firms, Eagle-Picher Industries, Inc. and Gould Inc. The objective is to identify near-term (1978-1985) markets that can support high-performance/high-cost batteries that can be produced in pilot-plant quantities. A preliminary report is expected to be completed in December 1976.

B. Systems Design

A systems-design effort now in progress is directed toward designs for a 30 kW-hr electric-vehicle battery and a truckable module of about 5 MW-hr capacity for a utility energy storage plant. The conceptual design for the 30 kW-hr electric-vehicle battery was described in the preceding quarterly (ANL-76-81, p. 26). The present effort is directed to the design of the cell prototype† establishing the cell configuration to be used in the design of the battery housing. A detailed design of the full-scale housing by Eagle-Picher Industries, Inc. is scheduled to begin in October 1976.

The conceptual design for the 5 MW-hr truckable module for a utility energy-storage battery was described in a previous quarterly report (ANL-76-35, p. 26-30). A preliminary design effort involving several groups from the battery program and mechanical and electrical engineering support from the Engineering Division of ANL is scheduled to begin the next quarter. The output from this effort is expected to define the cell and module configuration for the energy-storage battery to be tested in the BEST Facility, as well as the size and configuration of the battery modules to be tested during the next several years on typical load profiles for utility energy storage.

C. Industrial Contracts

1. Cell Fabrication

(R. C. Elliott, W. E. Miller, E. C. Gay, R. F. Malecha‡)

Three industrial firms--Eagle-Picher Industries, Inc., Gould Inc., and Catalyst Research Corp.--are participating in the development of Li-Al/FeS_x cells. Eagle-Picher is developing cold-pressing technology for the

---

*S. H. Nelson.

†Prototype of the cells that will be built for testing in the first full-scale 30 kW-hr battery.

‡Chemical Engineering Division, ANL.

fabrication of electrodes. Their efforts have resulted in a baseline cell design. Eagle-Picher is now concentrating on improving the specific energy and specific power of the cells. This is being done by incorporating selected design variables and electrode compositions into separate batches of cells. Positive electrodes of both FeS and FeS_2 are being developed, and the cells are fabricated in the charged state.

Gould is pursuing hot-pressing as the method for fabricating electrodes. The Gould program will emphasize the development of uncharged FeS_2 cells that are designed for operation on the upper voltage plateau ($FeS_2 \rightarrow FeS$). Catalyst Research is investigating the effects of manufacturing electrodes in a dry-room atmosphere, and is also developing a method for casting Li-Al electrodes.

Only Eagle-Picher has progressed into the second phase of the work. A number of cells of the baseline design were built and tested at ANL. The test results are presented in Section III.A of this report. Production of the second group of cells, described below, is now under way.

Eagle-Picher. As reported previously (ANL-76-81, p. 34), approval was given to Eagle-Picher Industries, Inc. to fabricate the balance of the FeS_2 cells under the original contract work statement. Both the positive and negative electrodes of these cells are made by cold-pressing powders. The electrodes are 12.7 x 12.7 cm, with thicknesses suitable for the intended application. The approval was given after a satisfactory method was devised for making a connection between the molybdenum terminal and the current collector of the positive electrode.

Under an addendum to the Eagle-Picher contract, approved in August 1976, Eagle-Picher will produce about 60 cells (12.7 by 12.7 cm) of nine different types; these cells are expected to have increased specific energy and specific power. Among the features to be tested are (1) Y_2O_3 felt separators, (2) Li-Al electrodes containing 55 at. % Li, (3) elimination of the negative electrode particle retainer, (4) larger current collector leads, and (5) offset current collector leads. Some of these features will be incorporated into the same cells. Cells are also being ordered for testing of three- and six-cell batteries. Eagle-Picher will build a 500-ton press that will provide the capability for conversion from 12.7 x 12.7 cm electrodes of 12.7 x 18 cm electrodes by early 1977.

Catalyst Research. A cell fabricated in dry air (<5 ppm water) at Catalyst Research Corporation was tested at their facility in Baltimore, Md. for more than 1600 hr. Cell operation was terminated owing to equipment failure. The cell data indicated slightly lower performance than that of a control cell for this test, which was fabricated at Gould Inc. The selection of a design not particularly suited to air assembly appears to have caused this lower performance. However, the absence of obvious adverse effects on cell performance is promising, and we are continuing to pursue this method of assembly. Cell testing was conducted in a sealed container (not a furnace well) that was internally heated and backfilled with an inert atmosphere. In many respects, this type of testing duplicates proposed battery operating conditions.

Catalyst Research Corp. is continuing the development of a cast Li-Al electrode. Three cells are being built and testing of these cells is scheduled to begin in October 1976.

Gould. A number of design discussions were held with Gould Inc. during the quarter, and a formal design review was held in August. The basic cell to be fabricated by Gould is an uncharged FeS cell with rectangular electrodes (12.7 x 17.8 cm). The positive electrodes, which have iron current collectors, are hot-pressed from a mixture of Li_2S, copper and iron powders, and LiCl-KCl eutectic salt. The negative electrodes are also hot-pressed, from a mixture of Li-Al (10 at. % Li) and LiCl-KCl powders.

The Gould cells contain a number of design features that will be examined for the first time. For example, in three cells, calcium will be added to the negative electrode to test its effect on cell lifetime. A new, improved feedthrough will also be tested in these cells. Gould is fabricating six prototypes, four will be delivered to ANL for testing and two to be tested at Gould.

2. Electrode Separators
(J. E. Battles)

The development of electrode separators to meet our technical and cost goals is being pursued under R&D contracts as summarized below. Related laboratory work is presented in Section IV.A of this report.

The Carborundum Co. Development efforts on BN bonded paper separators are being continued to define the process parameters for obtaining uniform bonding and for controlling fiber distribution, pore size, porosity, and thickness of the separator. Carborundum is preparing a detailed work breakdown for an extension of this contract (about six months) to allow for completion of these development efforts. A separate contract has been issued for the acquisition of 600 lb of BN to be stockpiled at the rate of 40 lb per month. An accountability procedure has been established to safeguard this material.

University of Florida.* Additional separator sheets consisting of 16% BN fiber, 4% asbestos fiber and MgO powder are being prepared. These sheets will be tested as insulators for the edges of electrodes in prismatic cells with felt or paper separators. Efforts are continuing on setting up a continuous paper-making machine. Replacement parts and materials (BN and Y_2O_3 fibers) have been received. The pilot-plant run scheduled for September 1976 was delayed to allow the paper-making machine to be relocated.

Zircar Products, Inc. Prototype yttria felts from Zircar are currently being tested in full-scale prismatic cells. Although the test results in small cells were very good, an initial test in a prismatic cell was unsuccessful because of some design features of the cell. Efforts are continuing on initiating a development contract with Zircar for improvement in the mechanical properties of Y_2O_3 felt and also for the development of BN felts by their precursory process.

*Contract funded directly by ERDA.

Fiber Materials, Inc. Fiber Materials, Inc. has acquired BN roving from Carborundum which will enable them to carry out the development and evaluation of various paper-making concepts using various blends of fiber lengths and additives to improve mechanical properties of the fabricated sheets.

North Carolina State University. The emphasis of this contract, which is awaiting approval from ERDA, is on the development of porous, rigid separators and on basic studies of MgO and the effects of impurities on its compatibility with lithium.

3. Feedthrough Development
(K. M. Myles)

Ceramaseal. A ram-type electrical feedthrough is being developed in this contract effort. Initial designs that were tested previously proved to have excellent leak-tightness. The recent effort by Ceramaseal has been concentrated on reducing bulkiness and increasing the conductor size. Delivery of these feedthroughs is expected during October and evaluation will commence thereafter.

Coors Procelain. This contractual effort is directed toward developing a method for cold-pressing Y_2O_3 parts. Subsequent efforts will be devoted to development of a nonmetallic braze for the Y_2O_3 to be used in production of a feedthrough. Thus far, Y_2O_3 samples have successfully passed a 1000-hr compatibility test in an environment of Li-Al + LiCl-KCl. Recently received metallized samples are currently undergoing a similar compatibility test.

4. Computer Programs
(F. Hornstra, J. Zagotta,* S. D. Gabelnick†)

An industrial-participant contract with International Harvester (IH) started in August; participation will be on a part-time basis. The goal is to develop a computer program to serve as a load profile simulator and to make the program operational on an ANL computer. IH has an ongoing activity in developing computer modeling programs for battery-powered vehicles. The program incorporates the effects of control and power-train elements on the range and performance of electric vehicles powered by advanced batteries.

An IH internal report has been supplied by ANL, along with a print-out of the computer program. The program has been loaded on one of the ANL central computers through the local data link. Modifications have been made to accommodate the ANL processor and the program has been run. Our personnel are being instructed in program operation while subroutines to input the characteristics of the 30 kW-hr Li-Al/FeS_2 battery are being incorporated.

---

*Industrial Participant from International Harvester.

†Computer Programming Group, Chemical Engineering Division, ANL.

III. BATTERY ENGINEERING
(E. C. Gay)

Battery engineering efforts are directed toward (1) testing of industrially fabricated Li-Al/FeS_x cells, as single cells and in various battery configurations, and (2) improvements in electrode and cell design and fabrication methods. As improvements in cell design are demonstrated, these are incorporated as quickly as possible into the industrially produced cells. Battery components and testing equipment are also being developed.

A. Industrial Cell and Battery Testing
(W. E. Miller)

Lithium-aluminum/metal sulfide cells are being produced by industrial firms and are undergoing testing at Argonne. Standardized testing procedures are being established so that cells of different designs may be compared on a common basis. The results obtained are being used to develop improved designs for the next generation of cells. (One recent change is an increase in the ratio of active material to cell weight.) Cells are also being assembled into battery configurations and tested; the results obtained so far are only preliminary, but the work of building a battery for the electric vehicle has begun.

1. Testing of Contractor-Produced Cells
(R. C. Elliott, T. D. Cooper, P. F. Eshman, W. E. Miller)

In general, the performance of the contractor-produced cells has not been as high as that for the ANL-produced cells operated in the Cell Development and Engineering Group, because the ANL cells are in most cases based on a more advanced technology. Recent attempts to involve the contractors in this more advanced technology have been successful (see Section II.C). Prospects are good for meeting the cell and battery goals in the near future.

One of the variables in cell design is electrode thickness. In general the peak power density of electrodes increases as the thickness of the electrode decreases. However, the cell specific energy increases with increasing electrode thickness. Therefore, cells needed for high power tend to have thin electrodes and cells needed for energy storage tend to have thicker electrodes. Two types of cells are being made by Eagle-Picher Industries, Inc. in order to investigate this effect of electrode thickness. Type A cells have electrodes about 0.3 cm thick and Type B cells have electrodes about 0.6 cm thick.*

The cells presently being tested were produced by Eagle-Picher Industries, Inc. with electrodes fabricated by cold-pressing powders into honeycomb current collector structures. The cells have FeS_2 positive electrodes with molybdenum current collectors of improved design (ANL-76-81,

*Because the cells have two negative electrodes and one positive electrode, the positive electrode is considered to consist of two halves, each having the thicknesses given here. In the material that follows, this dimension is often referred to as the half-thickness.

p. 12). In one group of cells (Type B) the positive electrodes have a half-thickness of 0.63 cm and capacities of 156 A-hr; the negative electrodes each have thicknesses of 0.72 cm and a total capacity of 149 A-hr. The performance of a typical cell in this series is described below. A summary of the present cell tests is presented in the Appendix.

Cell EP-2B4 was operated for 130 cycles and about 1700 hr. The operating temperature was 430°C except from Cycle 24 through Cycle 45, when it was 400°C. During Cycle 45, when the temperature was raised from 400 to 430°C, the capacity increased about 0.2 A-hr per degree. When capacity was plotted *vs.* current, a linear relationship was obtained in the range from 11-35 A. For cell data at 400°C, the slope of a curve of capacity *vs.* current was -1.25 A-hr/A, and for data at 430°C the slope was -1.37 A-hr/A.

A comparison of the power capability of Cell EP-2B4 at 430°C (Fig. III-1) and at 400°C (Fig. III-2) shows a decrease with decreasing temperature. This decrease results from a 22% increase in cell series resistance at the lower temperature.

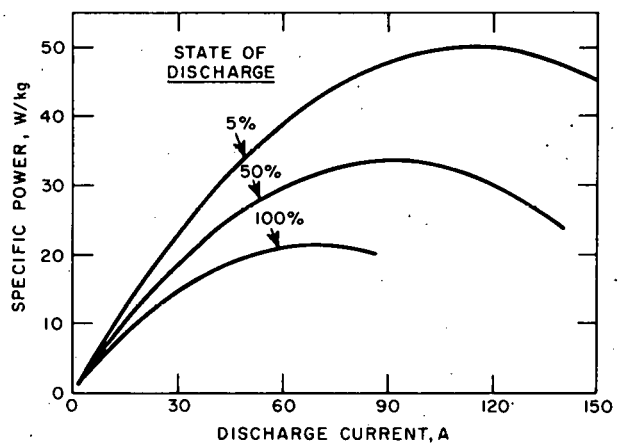

Fig. III-1.

Specific Power of Cell EP-2B4 at 430°C

Fig. III-2.

Specific Power of Cell EP-2B4 at 400°C

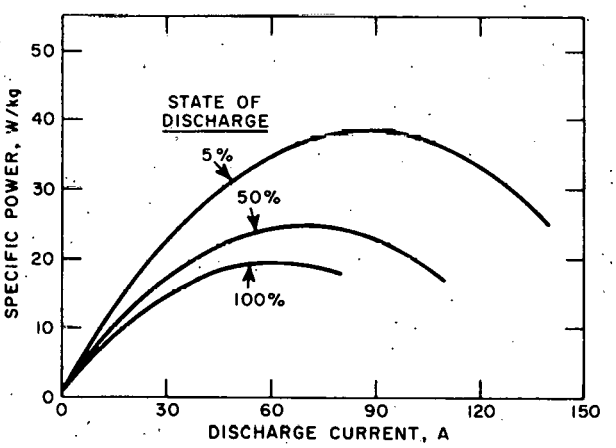

Figure III-3 shows the capacity of Cell EP-2B4 as a function of time. Values for specific energy shown on this curve reflect the changes in capacity and average discharge voltage. The cell was charged and discharged at essentially constant current density (42 mA/cm^2) throughout its life. In later cycles, much of the capacity could be restored by lowering the charging current. This behavior can be interpreted as a decreasing charge-acceptance capability. Therefore, we have begun a study of the effects of charging parameters on cell life. Results will be reported at a later date.

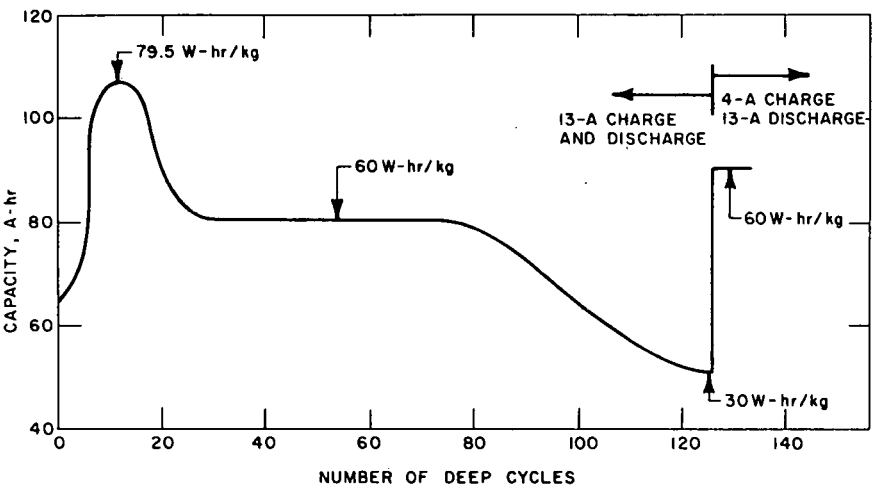

Fig. III-3. Cycle Life History of Cell EP-2B4

The construction of Li-Al/FeS_2 Type A (thin) cells is somewhat different from that of the Type B (thick) cells. The negative electrodes are each 0.33 cm thick with a total capacity of 34.4 A-hr. The positive-electrodes half-thicknesses are also 0.33 cm, and the total theoretical capacity is 35.2 A-hr FeS_2. Cell EP-2A5 is typical of this group of cells. In the first qualification tests, the specific energy of Cell EP-2A5 ranged from about 57 W-hr/kg at the 3-hr rate to 67 W-hr/kg at the 5.5-hr rate. The results of the first tests of specific power are shown in Fig. III-4. Except for periods when specific energy and specific power were being measured, the cell has been cycled at a 10-A (5-hr) charge-discharge rate. After 72 cycles and 910 hr of operation, the cell has shown a decline of about 7% from its peak performance (12th cycle, 55.3 A-hr, and 67 W-hr/kg at the 5.5-hr rate).

2. Automation of Qualification Testing
(R. C. Elliott, R. W. Kessie,* P. F. Eshman)

The present qualification testing of contractor-produced cells has proved to be very useful for comparison of the effects of cell-design variations. The basic tests generate two types of data. The first, which is a plot of specific energy *vs.* hours of discharge, is generated by progressively discharging the cell at higher currents than are used during "normal" cell

*Computer Group, Chemical Engineering Division, ANL.

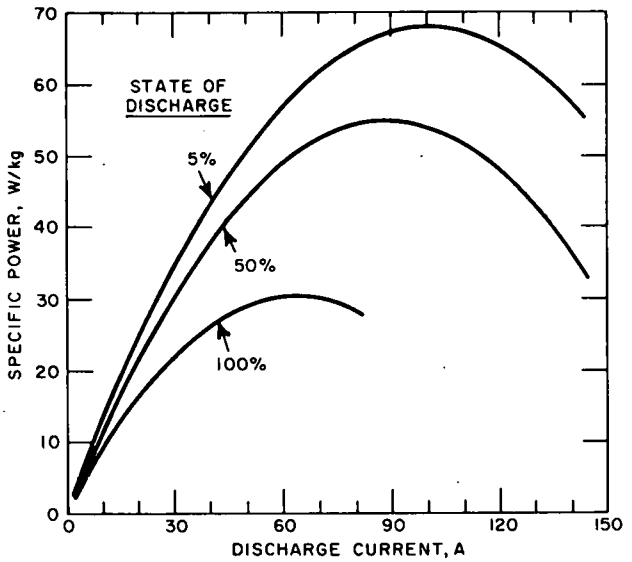

Fig. III-4. Specific Power of Cell EP-2A5

cycling. The second is a plot of specific power *vs.* current, as shown in Figs. III-1, -2, and -4. The specific power data are generated by manually applying 15-sec current pulses at progressively increasing currents and recording the cell voltage; the raw data are analyzed to generate statistical estimates of cell peak power, resistance, and open-circuit voltages.

The present tests, when implemented manually, are subject to experimental errors which can be eliminated by automation. We are in the process of installing the necessary hardware and software for automated testing using the available Varian-Vidar-Robicon system. With automatic cell cycling and data acquisition, the data base for evaluation of specific energy and specific power will be strengthened owing to the elimination of errors and the ability to acquire more extensive data.

3. Battery Testing

(V. M. Kolba, G. W. Redding, J. L. Hamilton, E. C. Berrill*)

Battery testing efforts are directed toward the development and evaluation of battery configurations and designs. In this effort, the performance of cells in series and parallel arrangements is being evaluated, start-up and conditioning methods are being investigated, and charging procedures are being developed. Testing of these battery configurations is presently under way, with thick (Type B) FeS cells being tested for utility energy storage applications and thin (Type A) FeS_2 cells being tested for electric vehicle applications.

Testing of cells in both parallel and series arrangements is required to fully understand the interactions of the cells and to establish baseline data for scale-up of battery designs. In all present battery designs for both applications, cells are arranged in parallel-series configurations; the parallel connections provide increased capacity and the series connections

*National Battery Test Laboratory Group.

provide increased voltage. To date, cells have been tested separately in both parallel and series arrangement. When sufficient cells become available, testing will be conducted in parallel-series arrangements. Thus far, cells have been individually monitored for voltage, and charge or discharge is terminated when one individual cell of the battery configuration reaches its voltage limit. When the cells are matched in capacity, the same cell reaches the charge and discharge voltage limits and therefore limits the battery capacity. However, when cells are mismatched, different cells may reach the limits, thereby causing a continuing decline in performance of the battery.

A description of the batteries and a summary of their operating characteristics are presented in the Appendix; the effects of charge and discharge rates on performance are illustrated in Table III-1. In the discussions of performance presented below, the specific energy and specific power values are calculated on the basis of combined cell weights. In the tests, constant IR-included cutoff voltages are used. This procedure results in a more pronounced decline in capacity with current than for constant IR-free cutoffs, because the increased polarization that results from higher current is not compensated for.

Table III-1. Summary of Battery Performance at Various Charge and Discharge Rates

Batt. No.[a]	Cell Type[b]	Theor. Cap., A-hr	Cutoff Voltage,[c] V		Performance at Indicated Rate				
					Rate, hr		Cap., A-hr	Eff., %	
			Discharge	Charge	Discharge	Charge		A-hr	W-hr
B6-S	FeS, thick	149	1.1	1.56	7.6	7.6	76	99	83
B7-S	FeS, thick	149	1.0	1.56	23.4	23.4	117	97	79
					10.0	8.5	100	99	78
					5.1	6.2	77	98	74
					2.8	4.1	57	99	72
					1.4	3.5	35	98	69
B8-P	FeS_2, thin	149	1.0	2.0	5.8	5.8	113	99	83
					1.9	4.5	90	99	68
B8-S	FeS_2, thin	69	1.0	2.0	5.0	5.0	50	99	78
					2.2	4.3	43	99	66
					0.7	3.0	22	98	53
					2.0	4.0	21[d]	98	64

[a] S = series, P = Parallel. Three cells in B6-S, two cells in remainder.

[b] All cells fabricated by Eagle-Picher.

[c] Cutoff voltages are for all tests and are IR-included.

[d] Short cycles; 1-hr discharge at C/2 rate.

a. Testing of Thick FeS Cells

During this period, testing of Cells EP-1B4, -1B5 and -1B6 in series (designated Battery B6-S in ANL-76-81, p. 31) was terminated after the 14th cycle because of declining capacity and poor ampere-hour efficiency. Cell EP-1B5 was removed from the group because of a 4-A leakage current; the cell is undergoing a post-test examination.

Testing of Cells EP-1B4 and -1B6 in series, now designated Battery B7-S, was continued. The effects of changes in voltage limits and the use of equalization after each cycle were investigated, and discharge rate and power tests were also conducted.

Initial testing of B7-S was performed with voltage limits on discharge and charge of 1.1 and 1.56 V, respectively, to permit comparison with individual cell data. These limits were changed to 1.0 and 1.59 V with an attendant increase in achievable capacity of ∿12%. The changes in voltage limits and the use of equalization at the end of the bulk charge cycle increased the achievable capacity by 35%, yielding an achievable specific energy of ∿62 W-hr/kg at a 10-hr discharge rate, as shown in Figure III-5a. The 10-hr discharge rate was the original design basis for load-leveling application. At the 5-hr discharge rate, which is representative of the peaking application, the specific energy was ∿43 W-hr/kg. Operation of a battery for peaking purposes would require a modification in design to achieve higher specific energy at shorter discharge times. Data from the power tests are shown in Figure III-6. A peak specific power of ∿17 W/kg was obtained at 50% discharge at a current of 50 A.

Testing is being oriented toward establishing rates permitting a 5-hr discharge and 10-hr charge, including ∿4 hr of equalization.

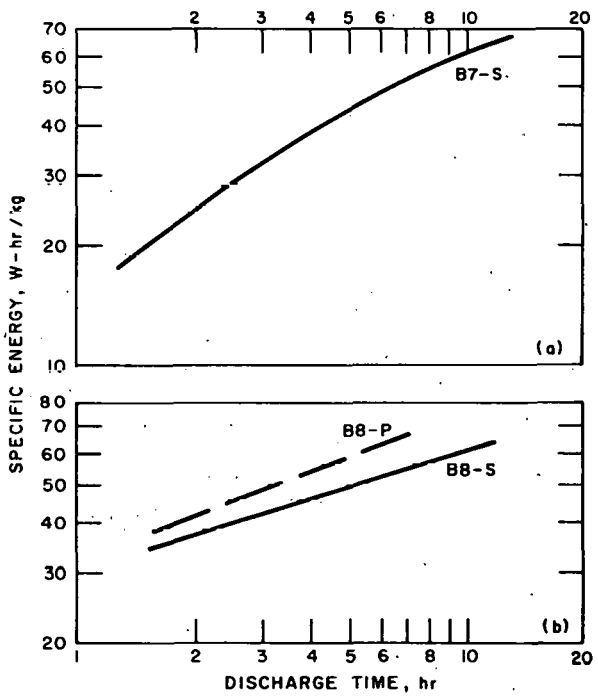

Fig. III-5.

Specific Energy *vs.* Discharge Time for Batteries B7-S, B8-P, and B8-S

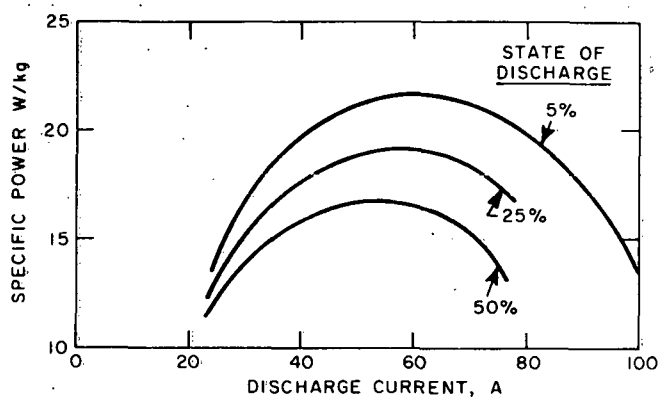

Fig. III-6. Specific Power of Battery B7-S (measured at the end of 15-sec pulses)

b. Testing of Thin FeS_2 Cells

A method for start-up and conditioning of many cells, prior to battery assembly and operation, may be important to our program from the standpoint of available time and equipment. A review of two possible arrangements (series or parallel) for cell start-up and conditioning indicates that the parallel arrangement is advantageous from the standpoint of control of cell voltage levels. This method was tested using two thin-type FeS_2 cells (EP-2A3, -2A4). The cells were clamped together (using a mica separator in areas requiring electrical insulation), placed in a test well, started up, and conditioned in a parallel arrangement designated B8-P. Data from this battery were compared with data from Cell EP-2A5, which is being cycled individually in a glove box. The peak capacities achieved for the cells in B8-P were within 1% of those for Cell EP-2A5, while the specific energy and specific power values were within 10%. This method will allow many cells to be readily and reproducibly conditioned at one time.

After the conditioning procedure, tests of Battery B8-P were conducted to determine specific energy, energy efficiency, and coulombic efficiency at various discharge rates; power tests were also conducted. Results of the specific energy tests are shown in Fig. III-5b. At the 5-hr rate (original design base) the specific energy is ∿59 W-hr/kg, while at the 2-hr rate it is ∿43 W-hr/kg. Figure III-7 shows the data from the power tests at 25 and 50% discharge (the data for 5% discharge, not shown, were within 3% of those at 25% discharge). At 25 and 5% discharge, the peak specific power of ∿67 W/kg was attained at a current of ∿220 A. At 50% discharge, the specific power was ∿51 W/kg at ∿200 A. After the power tests, the resistances of the cells had each increased from ∿7.5 to ∿12-16 mΩ. In the post-test analysis of these cells, an attempt will be made to identify the cause of these increases.

After 30 cycles of parallel operation, Cells EP-2A3 and -2A4 were connected in a series arrangement, designated Battery B8-S. After this battery was cycled to develop a data base, high-rate discharge and power tests were conducted. Also, the effects of equalization, charge rate, voltage limits and short-cycle operation (for 1 hr at the 2-hr rate) were investigated. Test results of specific energy *vs.* discharge time are shown

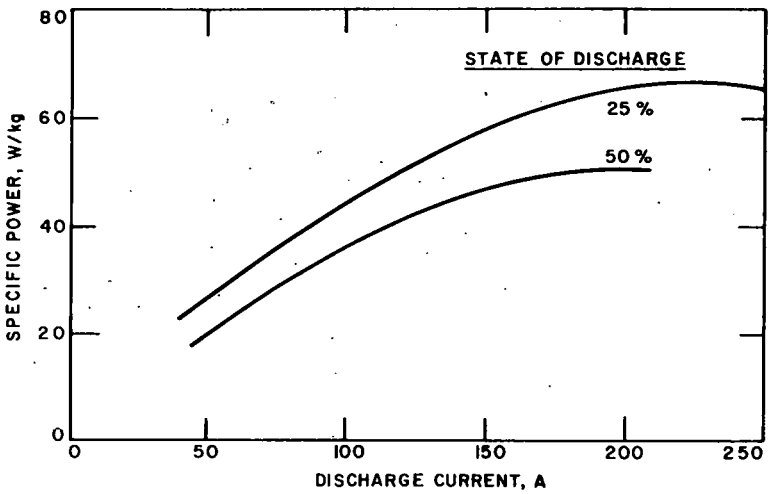

Fig. III-7. Specific Power of Battery B8-P (measured at the end of 15-sec pulses)

in Fig. III-5b. The performance of B8-S was lower than that of B8-P because of the resistance changes in the cells and the increase in resistance of cell interconnections. At the 5-hr rate, the achievable specific energy of B8-S was ∿49 W-hr/kg, while at the 2-hr rate it was ∿37 W-hr/kg. The specific power of ∿37 W/kg was attained at 5% discharge; at 50% discharge, a specific power of ∿25 W/kg was attained.

Short-cycle testing of B8-S was conducted to determine the effect of cycling for 1 hr at the 2-hr rate of discharge. This mode of operation lowered the energy efficiency slightly (∿6%) compared with the value for deep discharges at the 2-hr rate. As cycling progressed, the achievable capacity of B8-S slowly decreased at a rate of ∿0.37 A-hr per cycle. Various methods of restoring the capacity were investigated. Most of the former capacity could be restored by 1) constant current charging at a lower current (longer time), 2) equalization, or 3) increasing the charge cutoff voltage limit. Some success was also obtained by a current-limited constant-voltage charge, which yielded higher achievable capacity on the succeeding discharge than that obtained after a constant-current charge alone. This method will be more fully explored upon completion of a control mechanism required for cycler operation in this mode.

As part of the testing described above, a Gulton equalizer designed for FeS_2 cells (see Section III.B) was used to equalize the cells. Use of this equipment required long times for equalization (maximum current achieved, ∿0.9 A). A 19-hr equalization increased the capacity and energy on the subsequent cycle by 12.7%.

Test cycling schedules are being prepared that provide for discharge of cells at various rates and depths of discharge. Tests performed according to these schedules will provide the necessary data for evaluating the cell performance with respect to the goals for both the electric vehicle and utility energy storage batteries.

4. Cell Testing Facilities
(I. O. Winsch, R. F. Malecha, W. E. Miller)

The design of a multicell test heating chamber was completed and a 25-kW unit with appropriate controls has been ordered. This unit, which is designed to heat eight experimental cells simultaneously under an argon atmosphere at 450°C, will be used in evaluating the performance of contractor-produced cells. Cells with dimensions from 13 by 13 cm to 20 by 20 cm can be conveniently heated and tested in the heating chamber. Receipt of the multicell heating chamber is scheduled for November 1976.

Four cylindrical heating chambers, which will be used for heating and testing contractor-fabricated cells, have been installed. Each unit is capable of containing a cell 13 by 18 cm or 20 by 20 cm, and the units are individually heated. A helium-atmosphere glove box, now being modified will be installed for storing contractor-fabricated cells and cell parts. A larger glove box will also be installed for housing an electrolyte-filtering system, pulverizer, and sieving unit.

B. Battery Charging Systems

1. Electronic Development
(W. W. Lark, J. L. Hamilton, C. Russell*)

A six-cell monitor/controller has been assembled, and check-out of the unit is under way. The system is more sophisticated than the four-cell monitor/controller presently in use. In the six-cell unit, sensing of the upper voltage limit is inhibited during equalization so that the desired cutoff voltage for equalization may be set without interfering with the normal operation of the monitor; as a result, individual status lamps display only the information related to the main charge and discharge portions of the cycles. Sensing of cell voltage is also prevented during charge/discharge transitions of the main cycle to preclude the transition current spikes from falsely signaling the monitor. Other refinements are included to make the system simpler to use.

A mini-cycler was modified to provide a means for pulse-charging Li/FeS cells in experiments of the Cell Chemistry Group. The output current of the mini-cycler follows a desired waveform provided by a standard function generator, as programmed by the user.

2. Battery Charging Systems for Electric Vehicles
(J. Cox,† F. Hornstra)

A charging system suitable for mass-produced electric vehicle batteries must be economical, lightweight, reliable, and simple to use. Such a charging system requires two separate chargers. The first device, a high-current main charger, supplies the bulk of the battery charge at a maximum current that is limited either by the capability of the battery to receive current or by that of the power supply to deliver current. The second unit,

*Co-op Student from University of Cincinnati.

†Industrial Participant from Gulton Industries, Inc.

a charge equalizer, supplies the required difference for the low cells plus whatever charge the high-current charger did not supply.

The minimum cost (and minimum weight) charge equalization system charges comparatively slowly; therefore, it is desirable to utilize the high-current main charger to the greatest extent feasible. To minimize the costs of this high-current charger, a computed relationship between current and allowable battery voltage, based on demonstrated models of cell behavior, was assumed. The main charge current is progressively reduced, in several steps, as the cell voltage limit for the predicted "worst case" is approached. The final step in the main charge program occurs when the current has been reduced to a value near that available from the charge equalization system. Thereupon, the charge equalization is introduced to complete the charging process.

A complete charging system is illustrated in Fig. III-8. The main charger is controlled by the battery voltage, as indicated above. The equalizing charger utilizes small tap wires permanently connected to the junction between adjacent battery cells. At the specified voltage level, the main charge is terminated and the equalizer charge completes the process. The equalizing charger provides an independent, current-limited, constant-voltage source to each cell, so that each cell may come to a full charge independently. The unique diode arrangement depicted allows a reduction in the number of transformer secondaries (each secondary winding serves two cells) and eliminates cell-to-cell interaction due to lead wire resistance. This system was designed to provide effective cell charge equalization during a weekend battery charge.

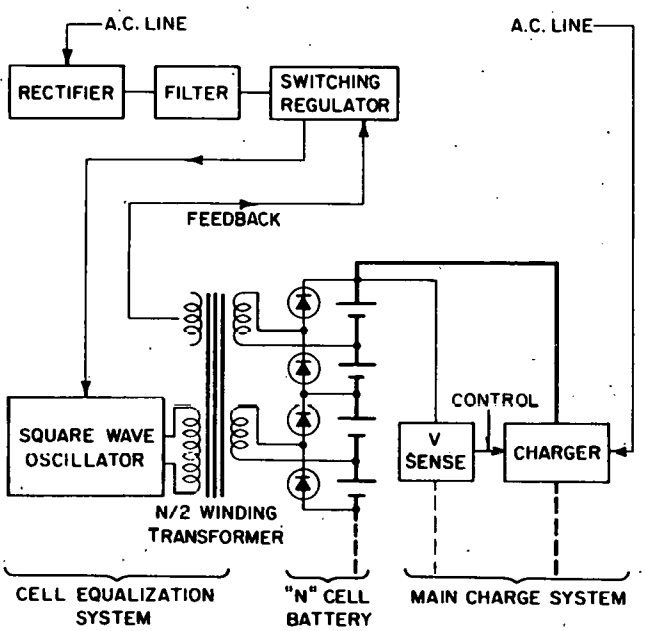

Fig. III-8. Charging and Cell Equalizing System for an Electric-Vehicle Battery

a. Present Status

Two prototype six-cell charge equalization systems (one for FeS cells and the other for FeS_2 cells) of the basic design shown in Fig. III-8 were constructed by Gulton and tested. The units provided independent cell charging and excellent regulation of the charge cutoff voltage. Although the initial charging currents are somewhat less than expected from the design specifications, the basic concept of the approach appears valid.

Components used in the construction are inexpensive. The diodes are those commonly in automobile alternators and are therefore mass-produced, readily available, and inexpensive. It is expected that a full-scale equalizer for electric-vehicle application can be mass-produced for about one dollar per cell.

b. Future Program

For the next phase of the program, the following activities are being considered: (1) construction of a full-size equalization system suitable for the 30 kW-hr electric vehicle battery, (2) design of a main charger for the 30 kW-hr electric vehicle battery, and (3) design study of a charge equalization system suitable for charging on a daily basis.

The full-scale equalization system, which will be a scaled-up version of the six-cell prototype, will be constructed under a contract. Emphasis will be placed on making the full-scale unit compact, while retaining much of the versatility that was built into the prototype systems.

The design of the main charger requires further study before construction can proceed. An industrial development contract will be negotiated to include the study, design, and construction of a full-size prototype main charger with a charging profile matched to the computed relationship between allowable current and battery voltage.

Finally, a contract will be initiated to study the requirements for charge equalization on a daily basis and to design a system to perform this duty. If the study indicates that a significant improvement in performance is achievable at an attractive cost, the construction of a prototype unit for several cells may be undertaken.

3. Automatic Repair of a Battery Cell with an Open Circuit
(F. Hornstra, E. C. Berrill, S. Faist*)

A brief study was conducted on the application of copper-oxide electric cutouts to automatically bypass an open cell in a battery. As reported in the preceding quarterly report (ANL-76-81, p. 30), the bypass fusing would establish a current path around the cell so that the battery could continue to function at essentially the same voltage (*i.e.*, decreased by that of only one cell). As a result, the necessity for penetrating the jacket of a high-temperature battery to effect a repair would be eliminated or postponed to a more opportune time.

*Sweet Briar College Student Participant, Summer Undergraduate Research Program, coordinated by the Argonne Center for Education Affairs.

Some of the parameters and mechanisms which contributed to experimental observations made with commercially available copper-oxide cutouts were identified. Manufacturers of these devices were contacted and pertinent documents are being collected. The companies appear interested in this application; however, several problems need to be explored regarding the use of copper-oxide material at the currents and the temperature required. In particular, little information is available at the temperature of interest (~500°C). Other possible materials for this application were identified, namely, aluminum alloys and platinum alloys. Further study and development of various materials for use at the temperature of interest would be needed before the scheme could be applied successfully to high-temperature batteries.

C. Cell Development and Engineering
(H. Shimotake)

The effort in this part of the program is directed toward the development and testing of Li-Al/FeS_x cells having improved performance and lower cost. Any technical advances will be incorporated into the cells that are fabricated by industrial firms to complement the effort on commercial development. The work is presently concentrated on the development of two major types of positive electrodes, hot-pressed electrodes and carbon-bonded electrodes. Both charged and uncharged negative electrodes are being studied; the use of metal additives to the Li-Al electrodes is also being investigated. Cells utilizing these electrodes are critically evaluated from the viewpoint of performance, lifetime, fabrication methods, materials, and cost in order to select the most suitable designs for the next-generation cells.

Dimensions of electrodes in the test cells are 12.5 cm by 12.5 cm, except for special-purpose cells. A summary of performance results of the test cells is presented in the Appendix.

1. Cell Performance and Lifetime Improvement

a. Uncharged Cells with Hot-Pressed FeS_2 Electrodes
(L. G. Bartholme, H. Shimotake)

A series of cells will be built and operated to test the performance of hot-pressed uncharged FeS_2 electrodes. The first cell (R-15) has a molybdenum honeycomb structure in the positive electrode and pressed aluminum wire plaques in the negative electrodes and is designed to be operated on both voltage plateaus ($FeS_2 \rightarrow Fe$). The cell has been operated mostly at the 5-hr rate for 42 cycles and 650 hr; no sign of capacity decline has been observed to date, as shown in Fig. III-9. The cell has been operated intermittently at the 2-hr discharge rate; the frequency of the 2-hr rate tests will be increased later. The cell has a high internal resistance (20 mΩ) owing to a poor joint between the molybdenum central current collector sheet and the molybdenum terminal tab. An improved joint will be incorporated in the next cell, which will be an FeS_2 cell designed to operate on the upper voltage plateau ($FeS_2 \rightarrow FeS$).

b. Cells with Carbon-Bonded Metal Sulfide Electrodes
(T. D. Kaun, F. J. Martino, W. A. Kremsner)

Studies of three cells (KK-4, -5, and -6) with carbon-bonded iron-sulfide electrodes are continuing; these cells were described previously

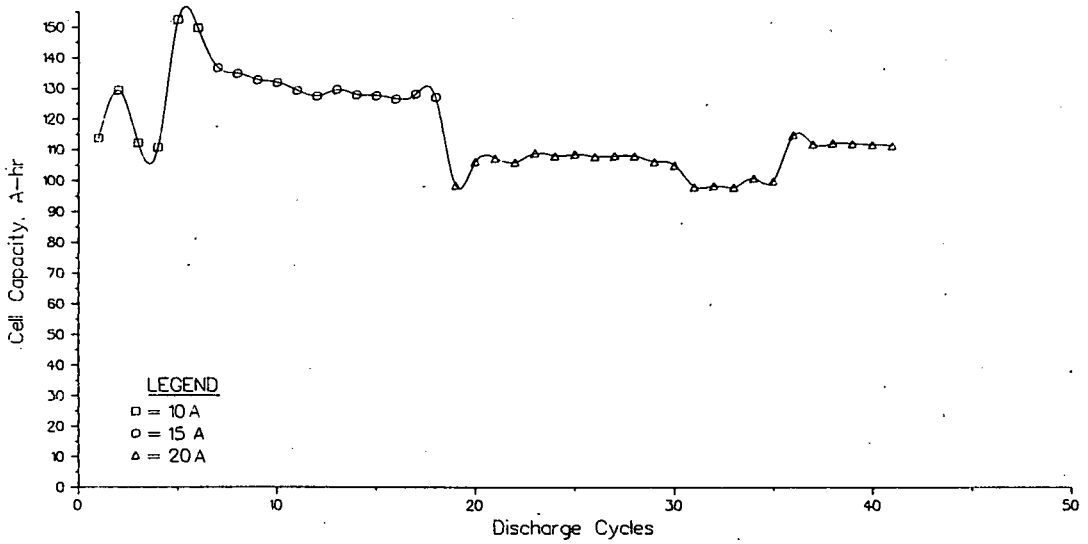

Fig. III-9. Capacity *vs.* Cycle Life for Cell R-15 (theoretical capacity, 168 A-hr)

(ANL-76-81, p. 13 and p. 16). Cell KK-4, a charged Li-Al/FeS_2-CoS_2 cell, has completed over 4600 hr and 280 cycles with an ampere-hour efficiency of >98%. The capacity of this cell has declined to 55% of its original value at a rate of 1 A-hr/100 hr of operation, as shown in Fig. III-10. A high open-circuit voltage (1.95 V) at full charge indicates a lithium-rich surface on the Li-Al electrode, which suggests that the cell capacity is limited by poor charge acceptance by the negative electrode. Attempts to improve cell capacity by varying the operating conditions have failed; long periods (18 hr) on open circuit with topping charges or rapid charge rates (100 mA/cm^2) for 10 cycles did not alter the rate of the capacity decline.

Cell KK-5, an uncharged Li-Al/FeS-$CuFeS_2$ cell, has maintained a low resistance of 3.8 mΩ since reassembly after an electrode examination (conducted after 1750 hr and 90 cycles). Its performance is stable, as shown by the data for capacity *vs.* cycle life in Fig. III-10. At the 5-hr rate

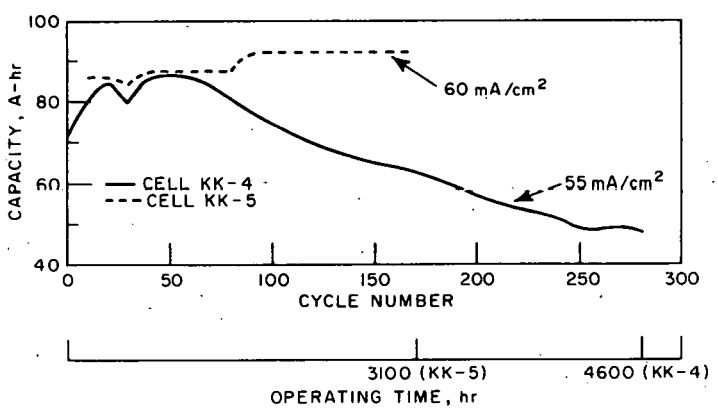

Fig. III-10. Capacity *vs.* Cycle Life for Cells KK-4 and KK-5 (theoretical capacities: KK-4, 90 A-hr; KK-5, 120 A-hr)

(60 mA/cm^2), the capacity is 92 A-hr (78% of theoretical), and at the 2-hr rate (130 mA/cm^2), it is 69% of theoretical (see Fig. III-11). The ampere-hour efficiency remains at 99% after 170 cycles and 3100 hr.

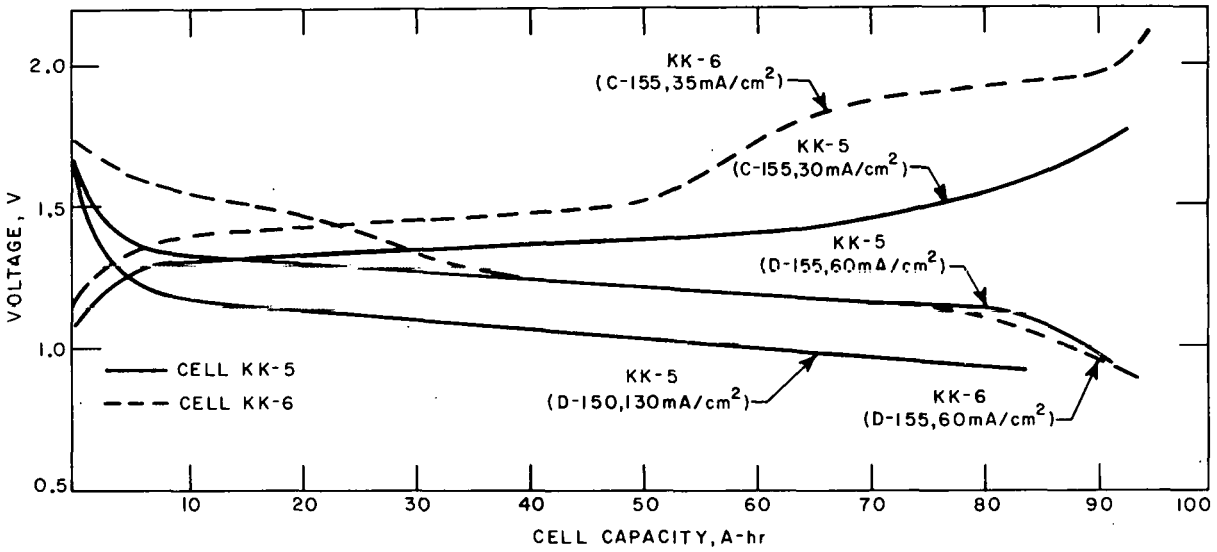

Fig. III-11. Voltage *vs.* Capacity for Cells KK-5 and KK-6 (theoretical capacities: KK-5, 120 A-hr; KK-6, 150 A-hr)

Cell KK-6, an uncharged Li-Al/FeS_2-CoS_2 cell, has operated for more than 2500 hr and 155 cycles at 99% ampere-hour efficiency. As evidenced by the voltage-capacity curves in Fig. III-11, Cell KK-6 never reached the fully charged state (150 A-hr). Cast plates of partially charged Li-Al (32 at. % Li) were used in the negative electrode to provide excess lithium capacity. A long period of operation (1500 hr and 100 cycles) was required for the negative electrodes to reach their present capacity of about 95 A-hr at the 5-hr rate. At the 10-hr rate, the specific energy is about 75 W-hr/kg.

Cell CB-1, a charged, Li-Al/$CuFeS_2$ cell with a carbon-bonded positive electrode and a hot-pressed Li-Al electrode has been in operation for more than 365 cycles and 5350 hr. The theoretical capacities of the electrodes are matched at 147 A-hr. The ampere-hour efficiency has remained high at about 98%, and the capacity is very stable with cycling, as shown in Fig. III-12. The cell has experienced no loss in capacity throughout its lifetime. This can be seen by a comparison of the capacities achieved in tests at the 7-hr rate, one ending at about Cycle 325, and the other ending at about Cycle 50. Moreover, plots of cell voltage *vs.* capacity at the 5-hr rate for Cycles 108 and 365 (see Fig. III-13) are almost identical, again illustrating the capacity retention of this cell. The capacity of 67 A-hr at the 5-hr rate represents a utilization of about 45%. The stable long-term behavior of this cell suggests that operation at a limited depth of discharge is a significant factor in capacity retention and long cell lifetime. This type of limitation would be practical for a utility energy storage battery, for which the specific energy requirements are much lower than for an electric-vehicle battery.

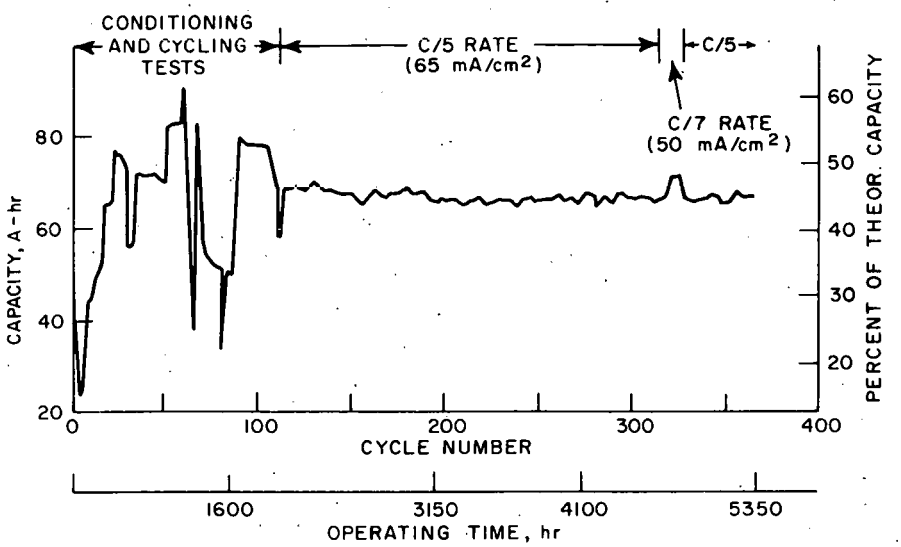

Fig. III-12. Capacity *vs.* Cycle Life for Cell CB-1 (theoretical capacity, 147 A-hr)

c. Multiplate Cells

Cells having multiple electrodes are being considered as a means of achieving high specific energy and low cell resistance. Two such cells, Cell MP-1 and -2, have been tested (ANL-76-81, p. 17). Operation of Cell MP-1 was terminated because of a leak in the cell housing.

Cell MP-2, comprises two carbon-bonded FeS_2-CoS_2 positive electrodes and four negative electrodes of Li-Al in iron Retimet. During 123 cycles and 1625 hr of operation, the cell capacity steadily declined. It was postulated that in a multiplate cell the cell performance is ultimately limited by that of the least efficient electrode and, consequently, electrode matching becomes extremely important. In an attempt to alleviate the problem in Cell MP-2, the cell was charged under constant voltage rather than under

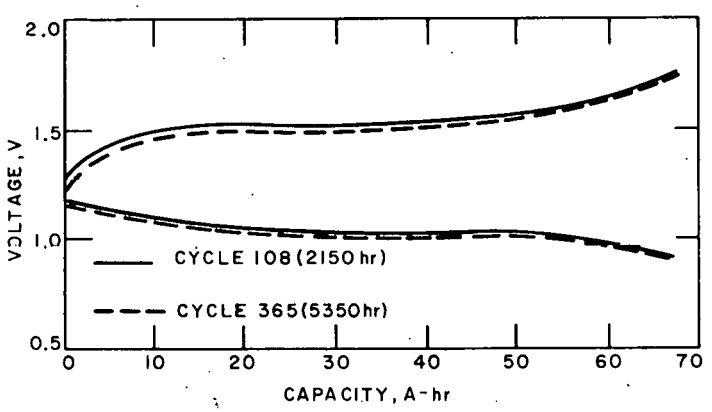

Fig. III-13. Voltage *vs.* Capacity for Cell CB-1 at C/5 Rate (theoretical capacity, 147 A-hr)

constant current. A high initial charging current followed by an exponentially declining current was considered to equalize the electrode capacities. However, after an additional 40 cycles and 300 hr of testing, performance data indicated that this method of charging had no beneficial effect on this particular cell. Next, the cell terminals were altered so that Cell MP-2 could be operated as two cells, each with one positive and two negative electrodes. Initial cycling showed that one of the positive electrodes was achieving a higher capacity than the other (35 A-hr compared with 15 A-hr). Since the connections were altered, the positive electrode with the lower capacity has shown increasing capacity with cycling. This behavior suggests that in the startup of this multiplate cell, one-half of the multiplate cell was conditioned preferentially. Improvements will be sought in the design of future multiplate cells.

2. Large-Scale Cell
(F. J. Martino, T. D. Kaun, J. E. Kincinas)

A large-scale (600 W-hr) cell, built on the basis of size recommendations established in the battery engineering effort for cells in the utility energy storage test program, has been in operation for 40 cycles and 750 hr. This cell (SS-1), which is 24 by 35 cm, has a charged, carbon-bonded FeS-Cu_2S positive electrode and two negative electrodes of Li-Al in iron Retimet, and a theoretical capacity of 650 A-hr. The objectives of this cell test are to evaluate 1) a cell having a carbon-bonded positive electrode of FeS and Cu_2S and negative electrodes of Li-Al in iron Retimet in a scaled-up design, 2) resistance and current distribution problems involved in scale-up, and 3) problems associated with the fabrication, handling, and start-up of electrodes of such large size.

In an effort to minimize degassing problems, the individual electrodes were placed between Inconel restraining plates and vacuum impregnated with electrolyte prior to cell assembly. Degassing was substantial but controllable. After the electrodes were removed from the electrolyte bath and cooled, the restraining plates were removed; no signs of warping or electrode misalignment were evident.

The cell was placed in operation at initial charge and discharge currents of 40 A (25 mA/cm^2); conditioning was accomplished in 10 cycles, which is typical for cells with vibratorily loaded negative and carbon-bonded positive electrodes. The cell resistance is very low, 1.4 mΩ. At the 10-hr rate, the cell capacity is 462 A-hr (71% of theoretical) and the energy output is 597 W-hr. The value of 71% utilization is at least as high as that achieved by any of the previous, smaller-scale test cells. Typical performance of Cell SS-1 at 25 mA/cm^2 (about a 10-hr rate) is illustrated in Fig. III-14. It is apparent from this cell test that a 5- to 6-fold scale-up does not alter the performance of this type of cell. Fifteen-second peak power testing will be conducted in the near future.

3. Electrode Development

a. Li-Al Alloy Negative Electrodes
(W. A. Kremsner, F. J. Martino, E. Chaney,* H. Shimotake)

Three types of Li-Al alloy negative electrodes were investigated in this period in an effort to achieve improved cell lifetime. The

*Industrial Participant from Gould Inc.

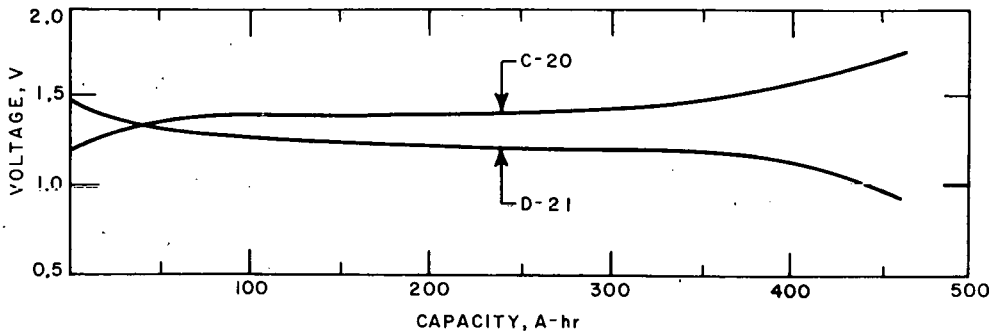

Fig. III-14. Voltage *vs.* Capacity for Cell SS-1 at 25 mA/cm^2 (theoretical capacity, 650 A-hr)

first type, made of a woven aluminum fabric having copper-coated steel strands* to improve current collection, was tested in Cell R-18, an uncharged Li-Al/FeS cell. Previous work has shown that the lifetime of Li-Al electrodes is strongly related to the amount of current collector in the electrode. The woven aluminum negative electrode may provide an inexpensive alternative to more expensive current-collector structures such as Retimet.† Cell R-18 had a hot-pressed positive electrode of FeS identical to that of Cell R-5 (described in ANL-76-9, p. 18). The cell has accumulated 62 cycles and 630 hr of operation, with the majority of cycles at the 5-hr rate. At this rate, the utilization of the cell is nearly 10% better than that of Cell R-5 at the same rate. This improvement may be attributed to the lower resistance (6 mΩ) of Cell R-18 having the new Al electrode, as compared with the resistance of Cell R-5 (20 mΩ). The test is being continued.

The second kind of negative electrode was a 50 at. % Li-Al alloy containing 0.6 at. % In and was tested in Cell FM-1, a charged Li-Al/FeS cell. Indium, among other materials, has been identified (see Section IV.B.2) as an effective additive in improving the lifetime of Li-Al alloy negative electrodes. These additive metals presumably prevent fragmentation of the Li-Al alloy by forming a ternary alloy during cycling. The Li-Al-0.6 at. % In alloy was vibratorily loaded into an iron Retimet current collector structure and operated against a charged, cold-pressed FeS-Cu_2S positive electrode; the positive electrode was a thick (Type A) electrode fabricated by Eagle-Picher and its performance characteristics were well-defined. After 30 cycles and 325 hr of operation at the 5-hr rate (8 A, 27 mA/cm^2), Cell FM-1 is showing stable performance with a capacity of 46 A-hr, corresponding to a utilization of 63%, respectively. No decline in capacity has been observed to date.

The third kind of the negative electrode was tested in Cell EC-1, an uncharged Li-Al/FeS_2 + CoS cell. In this cell, the negative electrodes were cast plaques of 25 at. % Li-Al alloy, giving about 50% excess lithium in the cell. One of the shortcomings of an uncharged Li-Al/FeS_x cell is that the cell capacity is limited by the negative electrode. The

*Product of National Standard Company; concept developed by K. M. Myles, Materials Development Group.

†A porous metal structure, product of Dunlop, Ltd., England.

use of a partially charged negative electrode such as 25 at. % Li-Al alloy would alleviate this shortcoming by providing additional lithium in the cell. Furthermore, the unused portion of the Li-Al alloy may provide additional current collection by forming a continuous, microporous network. Cell EC-1 was operated 11 cycles and 250 hr at 5-10 hr rates. Only one cycle at the 20-hr rate had been required to form the negative electrode before the cell could be operated at the higher rate. However, the cell developed a short circuit and the effect of the additional lithium on cell lifetime could not be determined. Further studies of this type of negative electrode will be pursued.

b. Li-Si Alloy Negative Electrodes
(L. McCoy,* L. G. Bartholme, H. Shimotake)

Although our present cell designs call for negative electrodes of Li-Al alloy, a Li-Si alloy is being considered as a possible alternative negative material. A charged cell (R-19) with Li_4Si alloy negative electrodes and FeS-20 mol % Cu_2S positive electrodes was operated to provide a direct comparison with data from previous tests of similar (R-series) cells with Li-Al alloy electrodes. The negative electrodes had rigid, compartmentalized structures filled with powdered lithium-silicon alloy containing 77 at. % lithium. The BN cloth separator was plasma-sprayed with $MgAl_2O_4$ to provide particle retention and to facilitate wetting with electrolyte. Cell R-19 has operated for 10 cycles and 150 hr. For the first cycles at low discharge rates, the Li-Si alloy cell has an energy output that is about 10% higher than that of a Li-Al alloy cell, because of the higher average voltage.

c. Carbon-Bonded Metal Sulfide Electrodes
(T. D. Kaun, W. A. Kremsner)

Carbon-bonded metal sulfide electrode structures provide a promising alternative to hot-pressed positive electrodes because of their potentially low fabrication cost and their good performance characteristics. These electrodes are made of a paste mixture of active material, graphite powder, an organic liquid binder, and a porosity agent, *e.g.*, $(NH_4)_2CO_3$, that is spread into a metal current collector. This mixture is cured and baked at prescribed temperatures. The resultant product is a porous carbon structure comprising active material and current collector. Electrolyte is introduced into the structure by vacuum impregnation. Because of the importance of the carbon binder, one of the key ingredients, several types of binders have been obtained and tests are being conducted in small cells to determine their effects on electrode conductivity and durability, and their chemical stability in relation to the cell products. In the first test, phenol-formaldehyde was used as the binder for the FeS-Cu_2S electrode; this electrode is being cycled versus a negative electrode of Li-Al alloy in iron Retimet. Tests of other binders are planned.

---

*Industrial Participant from Atomics International, Division of Rockwell International.

IV. TECHNOLOGY DEVELOPMENT
(R. K. Steunenberg)

A. Materials Development
(J. E. Battles)

Efforts in the materials program are directed toward the development of various cell components (*e.g.*, electrical feedthroughs, electrode separators, current collectors, and cell hardware), corrosion testing of candidate materials for these components, and postoperative examination of cells to evaluate the behavior of the various construction materials as well as that of the lithium-aluminum and metal sulfide electrodes.

1. Electrical Feedthrough Development
(K. M. Myles, J. L. Settle, E. Hall,* E. Chaney†)

The corrosive environment within Li-Al/LiCl-KCl/FeS_x cells precludes the ready adaptation of most commercially available electrical feedthroughs. The few that are compatible with the cell environment employ mechanical seals. At present, these feedthroughs are unacceptably bulky, and their seals lack sufficient leak-tightness. Accordingly, new and innovative brazed seals are being sought and, at the same time, work is in progress to minimize the shortcomings of the mechanical seals.

This ongoing effort, which has been reported in past semiannual and quarterly reports, has resulted in a modified Conax feedthrough that has been reliably used in all of the recent ANL cells and all of the commercial cells so far fabricated. A complete redesign of the Conax feedthrough is also under way that significantly reduces the cost, size, and weight of the feedthrough. The results of evaluation tests performed on prototypes were sufficiently encouraging that tooling was developed for assembling the feedthrough semiautomatically.

Recently, a study was made to determine the optimum conditions for sealing Conax compression-sealed electrical feedthroughs. Present commercial cells have Conax feedthroughs with 3/16-in. (0.48-cm) conductors, a boron nitride lower insulator, an Al_2O_3 upper insulator, and a bed of -325 mesh BN powder between the two insulators. The seal is obtained by compressing the BN powder layer with a packing nut which applies force to the upper insulator. The magnitude of the force is controlled by tightening the packing nut with a torque wrench. Present specifications call for the use of 6.3 ft-lb (8.5 N·m) of torque and 3.0 g of BN. Under these conditions, if one neglects the effect of friction, the compacting pressure on the BN powder is about 1300 psi (9000 kPa). A slightly greater force causes the lower BN insulator to break, thereby preventing any further compaction of the powder. Under the conditions specified above, the gas leakage rate through the assembled feedthrough is about 10^{-5} Pa·m^3/s.

The replacement of the weak BN insulator with a stronger ceramic body would allow the application of higher compacting pressures and would presumably upgrade the leak-tightness of the seal. Accordingly, insulators

---

*Student Aide, Howard University.

†Industrial Participant, Gould Inc.

of Y_2O_3 and BeO, both of which are resistant to the cell environment, were fabricated* for testing. (Corrosion tests of these materials are described in the following subsections.)

Before the Y_2O_3 and BeO insulators had been received and tested, the size and the operating current density of the prismatic cells were increased, thereby necessitating the use of 1/4-in. (0.64-cm) conductors in the feedthroughs. The powder bed for a 1/4-in.-dia (0.64-cm-dia) feedthrough has about twice the area of the powder bed for a 3/16-in.-dia (0.48-cm-dia) feedthrough.

A series of experiments was performed to establish the specifications for assembly of both types of feedthroughs. The test variables were the diameters of the conductors and of the feedthrough housings, the particle size of the BN powder, and the force for compressing the powder. The BN powder was either -325 or -48+325 mesh. The particle size distribution in the latter was 53 wt % -48+100 mesh, 32 wt % -100+200 mesh, 14 wt % -200+300 mesh, and 1 wt % -300 mesh. Under optimum conditions, leak rates of about 10^{-6} Pa·m^3/s could be obtained with either size feedthrough. The best results for the 3/16-in. (0.48-cm) conductors were obtained with -325 mesh BN powder and a torque of 50 ft-lb (68 N·m) on the packing nut (a pressure of about 13,000 psi, on 90,000 kPa, on the powder). The best results for the 1/4-in. (0.64-cm) conductors were obtained with -48+325 mesh BN powder and a torque of 150 ft-lb (203 N·m) on the packing nut (a pressure of about 15,000 psi, or 103,000 kPa, on the powder).

After conditions for assembling Conax-type electrical feedthroughs were optimized, a program was initiated to evaluate solder glasses as secondary sealants outside the primary BN powder seal. After the BN powder layer is compressed, the upper insulator is removed and a layer of solder glass (-100 mesh) particle size) is placed on top. The assembly is then heated to vitrify the solder glass and allow it to bond to the conductor and housing. So far, two types of solder glass (No. 1990 and No. 0150 from Corning Glass Works, Corning, N.Y.) have been tested. The 1990 solder glass was found to be unsuitable because it reacted extensively with steel. The 0150 solder glass is very promising because it bonds well to steel without extensive reaction. It is expected that bonding with 0150 solder glass will decrease leak rates of feedthroughs by several orders of magnitude.

2. Ceramic Materials Development
(W. D. Tuohig and J. T. Dusek)†

Rigid ceramic foams are currently being investigated for possible applications as battery separators. Foaming offers a technique for introducing higher levels of porosity into a solid body than are normally attained by the sintering of powders. Moreover, the process is economical and readily adapted to large volume production. Typical applications of ceramic foams are filters, lightweight aggregates in building materials, insulating refractories, and lightweight whiteware. Rigid foam is simply described as a

*Y_2O_3 insulators fabricated by W. D. Tuohig and J. T. Dusek, Materials Science Division, ANL; BeO insulators fabricated by National Beryllia Corp., Haskell, N.J.

†Materials Science Division, ANL.

dispersion of a gaseous phase within a solid material. The individual cells which comprise the void space may be almost totally isolated or highly interconnected, as in a sponge. Clearly the latter type is desirable for separator applications.

Yttria foams, to be evaluated as possible electrode separators, have been prepared from aqueous suspensions containing a commercial foaming agent* and a transient organic binder. Air is entrained by mechanical mixing. The suspension is then cast in a mold and dried. Drying must be done in a uniform manner to prevent cracking and segregation; drying in a partial vacuum has been used successfully. The dried foam is fired at temperatures of 1700-1800°C to produce the finished separator.

Figure IV-1 is a photograph at low magnification of an yttria foam that is approximately 92% porous. The cells appear to be multiply connected by large irregular channels. Figure IV-2 shows the porous microstructure of a cell. Developmental studies are being concentrated on control of the cell size and size distribution, and on optimization of organic additives. Foams which appear to have the desired structural characteristics will be characterized in terms of permeability to gas flow, liquid flow, and mechanical strength.

A second type of structure under consideration consists of coarse Y_2O_3 fibers which could be used in making separator mats. These fibers, shown in Fig. IV-3, are produced by extrusion of a plasticized Y_2O_3 powder mass through a 0.3-mm orifice. The green fibers are sufficiently strong to allow handling, thus permitting them to be pressed into a mat-like structure before firing. These fibers do not appear well-suited for paper making because of their size and fragility. They could be used, however, as a skeletal support which could be infiltrated to produce a desirable separator structure.

*Mearl Corp., Roselle, NJ.

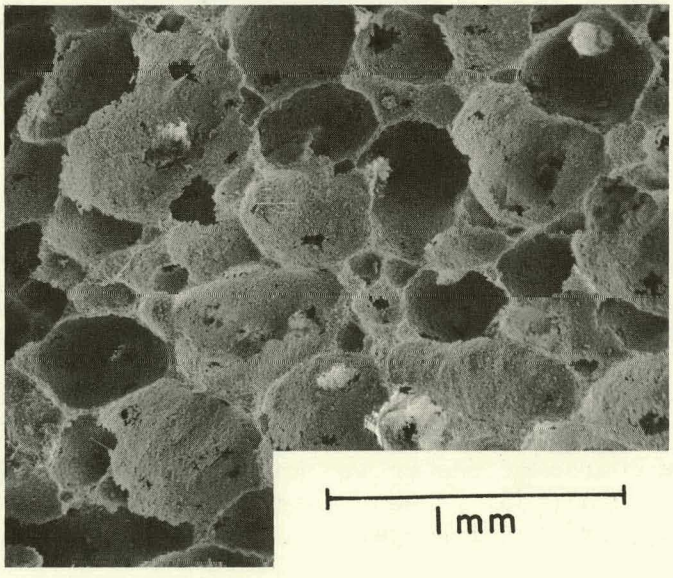

Fig. IV-1. Foamed Y_2O_3 Separators

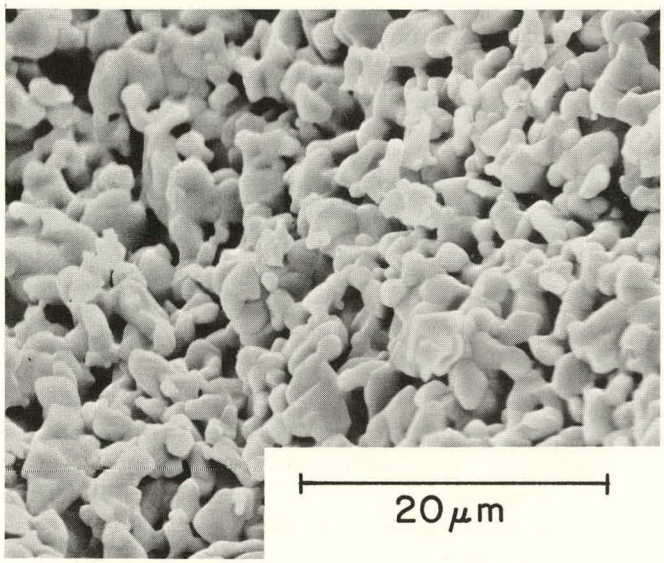

Fig. IV-2. Microstructure of the Cell Walls of a Y_2O_3 Foam

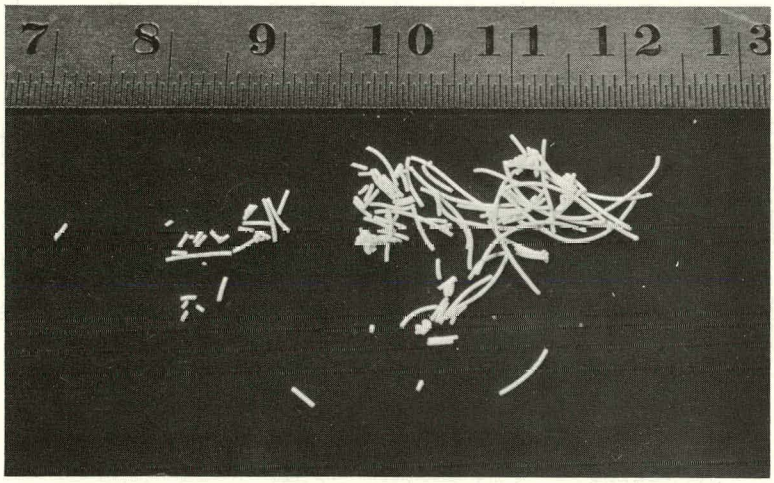

Fig. IV-3. Y_2O_3 Fibers Prepared by Extrusion

Insulators of commercial BeO* ceramic and Y_2O_3 prepared at ANL (see preceding subsection) were subjected to 5000-hr corrosion tests to determine their compatibility with the cell environment. Average rates of attrition based on weight loss were 30 μm/yr for BeO and approximately 3 μm/yr for Y_2O_3. Specimens were generally in excellent condition with no measurable change in gauge dimension. Metallographic examination did not show any evidence of grain boundary attack. Several specimens were observed to have cracked during the course of the test. However, the cracks appear to have originated from flaws already present in the material and resulted from machining, grinding, or drilling operations.

*K151, National Beryllia, Haskell, NJ.

3. Electrode Separator Development
(J. P. Mathers and T. W. Olszanski)

In the area of separator development, major effort is being directed toward paper and felt separators as alternatives for the BN fabric that is currently used in Li-Al/LiCl-KCl/FeS_x cells. The paper and felt separators are expected to be considerably less expensive than BN fabric and to provide more effective particle retention within the electrodes.

Scanning electron microscope (SEM) examinations were conducted on felts that had successfully withstood 1000 hr of in-cell testing (ANL-76-81, p. 19). The first material was a BN felt, developed by the Carborundum Company, which was bonded with BN. A post-test examination of this material by SEM showed no corrosive attack of either the fibers or the binders. The second material was an Y_2O_3 felt developed by Zircar Products, Inc., which required no binders. A post-test SEM examination of this material also showed no evidence of corrosive attack. However, some of the Y_2O_3 fibers were fractured, probably by the forces exerted on the separator by electrode swelling.

Most of the effort in this reporting period has been devoted to improvements in the separator test cell. Changes in the electrode containers have been made to avoid rupture during cell operation. Moreover, fabrication of the electrodes in the uncharged state was found to reduce out-gassing problems when the cell was put into operation, in agreement with the results of Shimotake and Bartholme.[2]

Separator tests have been started to evaluate the capability of the paper or felt separators to act as particle retainers. The first cell in this series, SC-12, was a Li-Al/LiCl-KCl/FeS cell assembled in the uncharged state. Yttria felt was used as the separator, with no particle retainers other than a layer of 325-mesh screen over each electrode face. (In initial cell tests, described above, particle retainers of ZrO_2 were used on the electrode faces, in addition to 325-mesh screens.) This cell was operated over 600 hr at a current density of 76 mA/cm^2, with a utilization of $\sim$50% and a coulombic efficiency of $\sim$100%. The cell has shown no signs of deterioration and operation of the cell will be continued until the 1000-hr test is completed.

4. Corrosion Studies
(J. A. Smaga, K. M. Myles)

Previous corrosion studies of candidate materials for current collectors in FeS_2 cells have been conducted in an equal-volume mixture of FeS_2 and LiCl-KCl eutectic, the most corrosive medium that these materials would encounter during cell operation. However, this condition exists only when the cell is fully charged, and thus the rates of corrosion do not reflect the less corrosive conditions of the positive electrode at intermediate states of charge. Corrosion tests have now been completed on selected materials in environments that simulated positive electrode conditions at 25, 50, and 75% discharge.

The materials for this test were prepared in small FeS_2 cells that were discharged to the desired conditions; the material was then removed

from the positive electrodes and analyzed prior to use in the corrosion studies. X-ray diffraction analysis gave the following results: at 25% discharge, $Li_4Fe_2S_5$ (Z phase) and FeS_2; at 50% discharge, FeS_2, Li_2S, Z phase, and $LiK_6Fe_{24}S_{26}Cl$ (J phase); and at 75% discharge, Li_2S and J phase. The materials evaluated were Hastelloys B and C, Inconels 617 and 625, and Type 304 stainless steel. In addition to the three mixtures representing the partially discharged electrodes, these materials were also tested in an equal-volume mixture of FeS_2 and LiCl-KCl eutectic. The tests were conducted at 450°C for 500 and 890 hr.

The corrosion rates declined sharply, as expected, with increasing depth of discharge. For Hastelloy B in the 890-hr test, the corrosion rates were 386, 107, +8.3 and 8.6 μm/yr for 0, 25, 50, and 75% discharge, respectively, and the corresponding rates for Hastelloy C were 595, 310, 10.3 and 5.5 μm/yr. The other alloys showed higher corrosion rates but still exhibited sharp declines with increasing depth of discharge. Examination of the samples showed a transition in the nature of the corrosive attack. Thick, well-developed sulfide scales were observed on the samples that had been exposed to FeS_2. For 25% discharge, samples which were exposed to a mixture of FeS_2 and Z phase still exhibited the FeS_2-type of scale formation but to a lesser extent. The attack on the samples at 50 and 75% discharge was similar to that in FeS-type environments, but the reaction rates were roughly two to four times higher. These higher rates are probably due to the presence of some FeS_2, which is more reactive toward these alloys than FeS.

The corrosion rates for a given environment and a given material were plotted as a function of the state of discharge. Each of the five curves was integrated over the discharge intervals of 0-25%, 25-50%, and 50-75% to derive estimates for the relative amount of corrosion occurring in each interval. These estimates are presented in Table IV-1. If one uses these values as the basis for predicting corrosion behavior under actual cell operating conditions, approximately 80% of the total corrosive attack on each of the four nickel-base alloys should occur in the first quarter interval (0-25% discharge). The remaining 20% of the total corrosion would occur in the next two intervals, mostly in the second interval (25-50% discharge). For Type 304 stainless steel, which is readily attacked by FeS_2, more than 95% of the total corrosive attack would occur in the first interval.

Table IV-1. Percent of Total Corrosion Occurring at Three Intervals of Cell Discharge

	Percent of Total Corrosion		
Alloy	0-25%	25-50%	50-75%
Type 304 SS	>95	>5	0
Hastelloy B	78.5	19.5	2
Hastelloy C	78.5	20	1.5
Inconel 617	83	16	1
Inconel 625	78	21.5	0.5

5. Postoperative Examinations

(F. C. Mrazek, K. G. Carroll, J. E. Battles)

Postoperative examinations are conducted on test cells primarily to evaluate the performance of various construction materials, in particular, feedthroughs, current collectors, electrode separators, and cell housings. These postoperative examinations provide important information, not only on the compatibility of cell components with the cell environment, but on the performance and behavior of the lithium-aluminum and metal sulfide electrode materials. The examination procedures were described in a previous semi-annual report (ANL-8109, p. 72).

a. Cells Fabricated at ANL

Postoperative cell examinations were conducted on four prismatic cells fabricated at ANL; two of these were assembled in the uncharged condition (S-86 and S-87) and two were assembled in the charged condition (BB-1 and 1B/F1). Brief descriptions of the cells and summaries of the metallographic observations are presented in Table IV-2.

Table IV-2. Results of Postoperative Examinations of Four ANL Prismatic Cells

Cell No.	Type of Cell	Total Operating Time, hr	Remarks
BB-1	Li-Al/ FeS-26 wt % Cu_2S	3493	The 0.08 mm mild steel honeycomb current collector used in both electrodes underwent considerable deterioration: >50% corrosion occurred in the positive electrode and Al alloyed with the steel in the negative electrode to a depth of 0.03 mm.
1B/F1	Li-Al/ FeS-26 wt % Cu_2S	334	First prismatic cell with Y_2O_3 felt separator. Movement of the positive electrode honeycomb current collector against the separator reduced its thickness by a factor of four or more.
S-86	Li-Al/ FeS_2-13 wt % CoS_2	5250	Current collector in the positive electrode was nickel sheet. Thickness of the sheet was reduced from 0.8 mm to 0.25 mm.
S-87	Li-Al/ FeS_2-13 wt % CoS_2	3460	Current collector in the positive electrode was Hastelloy B sheet. Thickness of the sheet was reduced from 0.4 mm to 0.3 mm.

A separator of yttrium oxide felt was utilized in Cell 1B/F1; this cell failed because of a short circuit after 15 cycles and 334 hr of operation at 430°C. Examination of the cell showed that the honeycomb current collector in the positive electrode had moved away from the central current-collector backing plate and was tightly pressed against the Y_2O_3 felt; as a consequence, the separator thickness was reduced by about a factor of four.* Metallic particles were observed in the middle one-third of the separator of this cell as well as in the separators of several other cells which utilized a copper sulfide additive. These particles were identified as metallic copper by electron microprobe analysis.† In areas where the separator was greatly compressed, owing to electrode swelling and the movement of metallic structural components such as current collectors or electrode frames, these metallic clusters can bridge the gap across the separator and cause numerous minor short circuits. This sequence of events is believed to have been responsible for the short circuit in this cell.

Cell BB-1 was identical in construction to Cell 1B/F1 except that the separator was BN fabric rather than Y_2O_3 felt; ZrO_2 cloth was used as a particle retainer in the positive electrode. Results of the examination of Cell BB-1 were similar to those of Cell 1B/F1, including the movement of the honeycomb away from the central current-collector backing plate in the positive electrode and the presence of copper particles in the separator.

The mechanism responsible for the presence of elemental copper particles in the separator is not known at this time. However, the morphology suggests that the mechanism involves a reaction in the electrolyte of soluble species such as Cu_2S (solubility, 1820 ppm at 520°C‡) and lithium to form Li_2S, which is also soluble to about the same extent as Cu_2S, and an insoluble product--in this case, metallic copper.

Cells S-86 and S-87 which had FeS_2 positive electrodes were operated to test nickel and Hastelloy B, respectively, as current collectors in FeS_2 electrodes. The nickel current collector in Cell S-86 showed irregular attack, presumably by the formation of a nickel sulfide, although no reaction layer was present. The Hastelloy B current collector in Cell S-87 retained a semiadhering reaction zone on the parent metal, which was fairly uniform in thickness across the surface.

b. Cells Fabricated by Industrial Firms

Postoperative examination of Gould Cell 02-006 provided an opportunity to investigate, for the first time, the effects of operation in an air environment. The cell, which was assembled in the charged state, had a negative electrode of Li-Al powder in iron Retimet and a positive electrode

*For comparison, examination of Cells EP-1B1 and -1B2 (ANL-76-81, p. 25) showed a much less extensive separation of the current collectors from the backing plates. In Cell EP-1B2, which was operated under mechanical constraints, the thickness of the BN fabric separator was reduced by about a factor of two; however, in Cell EP-1B1, which had no mechanical constraints, the reduction in thickness of the BN fabric was only about 10%.

†By W. A. Shinn, Chemical Engineering Division, ANL.

‡Solubility determined by James Hall, Undergraduate Participant, West Chester State College, West Chester, PA.

of FeS_2-CoS_2 in vitreous carbon foam. Boron nitride cloth was used as the separator material and ZrO_2 cloth as a particle retainer. During initial (336 hr) operation in a protective helium atmosphere, the cell output was abnormally low (utilization, ~20% of theoretical). Subsequently the cell was operated in air, for a total of 522 cycles and 3456 hr. No short circuits were encountered and testing was volumtarily ended with the cell fully charged.

The effects of air environment on cell operation appeared minimal. Iron oxide was formed on the outside of the steel case (0.75 mm thick) to a depth of 4 to 12 μm. Internally, the steel case showed no evidence of oxidation. The molybdenum positive-electrode current collector appeared to be unaltered by cell operation; the connection between the flattened molybdenum rod and the 0.15-mm molybdenum sheet was maintained only by the two rivets. The portion of molybdenum rod outside the cell seal showed no measurable loss of metal through oxidation. The feedthrough showed excellent electrical-insulation properties.

The electrodes of the cell were also examined. In the negative electrodes, the morphology showed an abrupt change from fine to coarse particles; the latter occupied about 75% of the electrode volume--the portion farthest from the positive electrode. The coarse particles are typical of the structure of the starting material, and their presence is consistent with the low utilization. Macroexamination showed that little electrolyte remained within the BN fabric separator; this circumstance probably contributed to the low utilization of the electrodes. In addition, microscopic examination showed the presence of large crystals of Li_2S within the central portion of the BN separators. Identification of the Li_2S was confirmed by X-ray diffraction and electron microprobe analysis.* Metallic iron particles were associated with the Li_2S. The presence of BN fibers within the larger Li_2S crystals indicates that they were formed *in situ* by a precipitation and growth reaction. Additional studies will be required to identify the mechanism responsible for this reaction.

B. Advanced Cell Engineering
(W. J. Walsh)

The relative merits of different types of advanced Li-Al FeS_x cells are being evaluated in an ongoing effort to identify the most promising directions for future work. The advanced engineering effort is presently concentrated on four areas: (1) studies of the mechanisms and causes of lifetime limitation, (2) studies of alternative binary and ternary lithium alloys, (3) development of large multiple-electrode FeS_2 cells for off-peak energy storage application, and (4) development of high-performance FeS_2 cells for electric-vehicle application.

Increased emphasis is being placed on the further development of Li-Al/FeS_2 cells that are operated on the upper voltage plateau ($FeS_2 \rightleftarrows FeS$; equilibrium voltage, 1.77 V *vs.* Li-Al). This design is being considered for the cells described in items 3 and 4 above. Upper-plateau cells appear to have a number of significant advantages: (1) very high power capability

*X-ray diffraction analyses by B. S. Tani, Analytical Laboratory, ANL; electron microprobe analyses by W. A. Shinn, Chemical Engineering Division, ANL.

throughout the discharge; (2) specific energies approaching those of two-plateau cells; (3) relative ease in adjusting the Li:S ratio in uncharged cells; (4) greatly reduced thermal energy dissipation during discharge; (5) greater protection from overdischarge; (6) simplified control requirements through the use of a single voltage plateau; (7) reduced conductor/connector weights because of the higher cutoff voltage and the resulting reduction in maximum battery current; (8) ease in fabrication (*i.e.*, no need for supplemental lithium in the uncharged negative electrode, and available methods for pressing uncharged upper-plateau FeS_2 electrodes); and (9) cost advantages associated with the higher average voltage. The major disadvantages of the upper-plateau FeS_2 cell are the need for molybdenum current collectors in the positive electrode, and the requirement of 50% more cobalt sulfide additive per kilowatt-hour of output than is required for two-plateau FeS_2 cells.

Previous work (ANL-76-81, p. 45) on electrolyte-starved cells showed that good electrical performance could be achieved initially, but declining capacity and increased polarization occurred after only a few cycles, apparently owing to migration of electrolyte away from the separator. The effort on this type of cell has been reduced pending the development of a separator with improved wetting characteristics. Similarly, the effort on "button" cells has been reduced because of the severe problems associated with seals and insulators in this type of cell. Both electrolyte-starved cells and button cells appear to be promising concepts for primary batteries, but many engineering problems would have to be solved before these concepts could be applied to secondary batteries, which require long lifetimes.

1. Multiplate Cell Development
(J. D. Arntzen, W. J. Walsh)

A multiplate cell (Li-Al/FeS_2, Cell A-1) incorporating several new design concepts was put into operation during this period. Cell A-1, which was assembled uncharged, contained three negative and two positive electrodes and was designed for operation on both voltage plateaus ($FeS_2 \rightleftarrows Fe$). The negative electrodes were pressed aluminum demister wire and the positive electrodes were a hot-pressed mixture of Li_2S, CoS_2, Fe, Li_2C_2 and LiCl-KCl.

The cell housing was designed with one side removable, so that the electrodes could be loaded through the open side during assembly. This feature eased the assembly procedure, facilitated welding of individual components to the housing, and allowed accurate spacing and good control of pressure between the electrodes during assembly. The positive electrodes were wrapped with ZrO_2 and BN fabrics so that all folds and overlaps occurred at the edges of the electrodes, thereby providing smooth, seamless layers at the active faces. The housing held the folded edges in place, and a restraining channel was used at the top of the positive electrodes together with a BN insulator (pressed against the BN cloth) to prevent active material from escaping from the top of the electrodes. The positive electrodes utilized a one-piece current collector/current lead/voltage lead made from 5-mil molybdenum.

The outer two negative electrodes were held in place by a 5-mil angle frame that was spot-welded to the cell housing at the edges of the electrodes. A 325-mesh stainless steel screen, welded to this frame across the face of the electrodes, was provided to contain the active material and prevent dendrite growth. The central negative electrode was enclosed in a lightweight "picture frame" having screens that covered both faces of the electrode. The "picture frame" was welded to a heavier bus, which was in turn welded to the cell housing.

Cell A-1 had a theoretical capacity of 426 A-hr and weighed less than 2.9 kg after it was filled with electrolyte. The cell was operated for 31 cycles and 1075 hr and achieved a specific energy of 110 W-hr/kg at the 8-hr rate. Figure IV-4 shows one of the early charge-discharge cycles, and Fig. IV-5 illustrates the performance of the cell as a function of cycle number. A summary of the cell performance is given in the Appendix.

The cell test was terminated because of a worsening short circuit. Postoperative examination revealed that the restraining channels at the top edges of the positive electrodes were inadequate and had become detached from the cell housing, thereby allowing the active material to extrude around the current lead and cause a short circuit. The negative electrodes were quite evenly reacted, with no indication of electrode mismatching. This cell design, with modifications, will also be tested in three-electrode configurations.

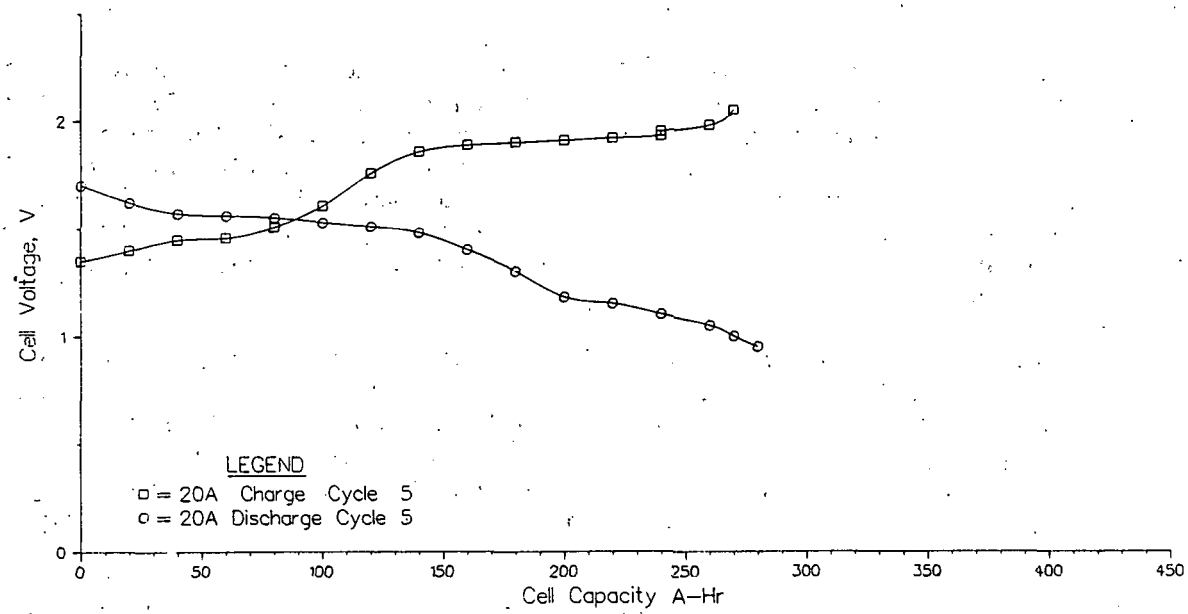

Fig. IV-4. Charge-Discharge Curve for Cell A-1 (theoretical capacity, 426 A-hr)

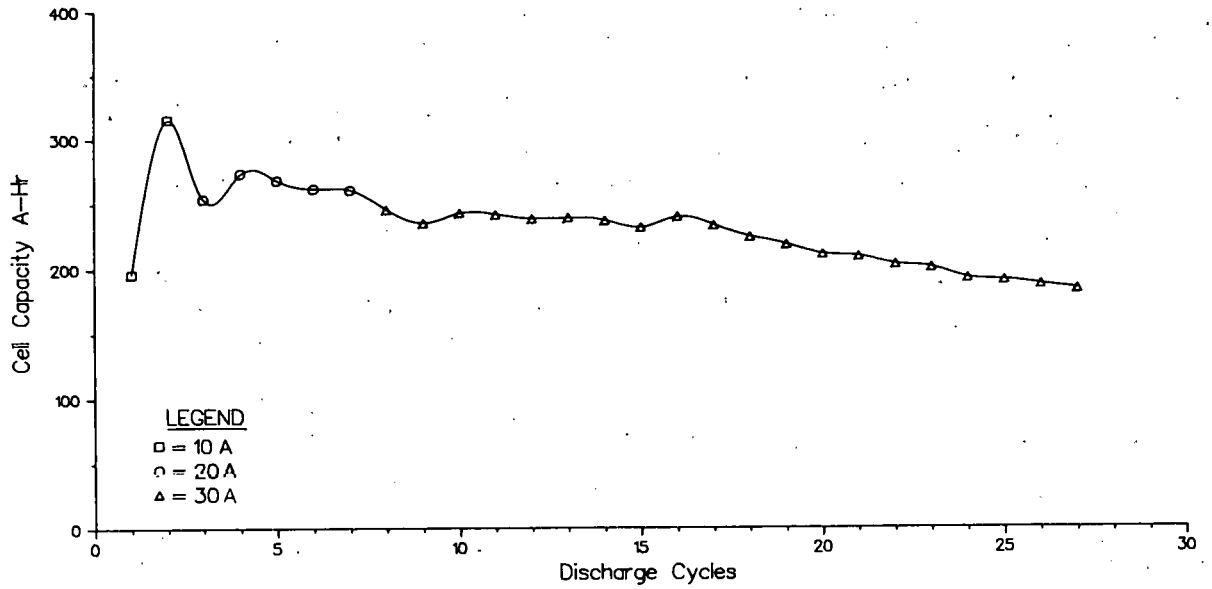

Fig. IV-5. Capacity *vs*. Cycle Life for Cell A-1 (theoretical capacity, 426 A-hr)

2. Advanced Electrode Development
(D. R. Vissers, K. E. Anderson)

Investigations are continuing on modifications of the Li-Al electrode that may result in sustained high capacities during extended cycling. It is suspected that the decreasing capacity of the present Li-Al electrodes results from morphological changes of the active material over a period of time. The present studies are focused on the use of various metallic additives to the binary Li-Al alloy as a possible means of controlling or modifying these morphological changes. The additives that are currently under investigation are indium, lead, and tin.

The Li-Al-M (M = metal additive) electrodes were prepared by melting mixtures of the desired composition at about 800-900°C in tantalum crucibles.* The alloy was ground to a powder and placed in an iron Retimet disk, which was enclosed in a 325-mesh stainless steel screen basket to contain the particulate material. This electrode, which had an area of 15.6 cm^2, was operated against a liquid-lithium counter electrode of the same area in LiCl-KCl electrolyte at ∿425°C.

The performance of the ternary-alloy electrodes was evaluated by comparing the capacity of the cells at constant current densities (0.05 to 0.10 A/cm^2 during charge and 0.05 to 0.30 A/cm^2 during discharge). The IR-free cutoff potentials for discharge and charge were 0.15 and 0.70 V, respectively; these are representative of the cutoffs for an upper-plateau FeS_2 cell.

*These materials were prepared by A. E. Martin of the Cell Chemistry Group.

Cell DK-33. The Li-Al electrode in this cell contained 3.9 wt % indium, and had a theoretical capacity of 10.27 A-hr. The performance of this cell was excellent. After an initial decline of about 5% during the first 100 cycles, the capacity remained constant until the 136th cycle, when the test was terminated. At the time of termination, the lithium utilization was 92% at the C/12 rate (0.05 A/cm^2) and 75% at the C/4 rate (0.10 A/cm^2). Further studies are in progress to determine the effect of the indium addition on the morphology of the active material and the concentration of indium required to achieve the desired effect. Although indium may not be a practical additive in the long range because of cost considerations, the results of this cell indicate that the addition of a third component to Li-Al electrodes may prolong their cycle life.

Cell DK-37. The Li-Al electrode in this cell contained 10 wt % lead as an additive and had a theoretical capacity of 7.78 A-hr. The performance of this cell was similar to that of a cell without the lead additive. The cell test was terminated after 120 cycles, at which time the lithium utilization was 74% at both the C/8 rate (0.05 A/cm^2) and the C/4 rate (0.10 A/cm^2). After 100 cycles, the lithium utilization appeared to be declining about 0.2% per cycle. These results indicate that the 10 wt % lead addition had little or no effect on the cycle life of the Li-Al electrode.

Cell DK-39. A test of a Li-Al electrode containing 4.9 wt % tin was recently started. Preliminary data from early cycles at the C/12 (0.05 A/cm^2) rate indicate a lithium utilization of 95%. Further results on this cell will be reported as they become available.

3. Lifetime Studies
(W. R. Frost)

The objectives of these studies are to determine the cycle life of the present Li-Al alloy electrodes and to identify those factors which limit cycle life. Cell LT-2 (ANL-76-9, p. 31), the second test in this series, utilized a Li-Al/LiCl-KCl/Al cell with Lithcoa electrolyte. The test was terminated as planned after 300 cycles and 4425 hr. The ampere-hour efficiency at termination was 99% and the lithium utilization was 46%. During the life of LT-2, the average lithium utilization was 52%. Postoperative analysis of Cell LT-2 indicated a buildup of lithium on the front faces of the electrodes and an axial concentration gradient of lithium in the electrodes. Evidence of the formation of a liquid-metal phase rich in lithium was also observed at various locations within the cell. Examination of the crystal morphology of the frozen electrolyte from the cell indicated that the electrolyte was no longer of the eutectic composition in many areas of the cell. This observation suggests the possibility that in these areas the electrode materials were coated by solid electrolyte during cycling and thereby became inactive. Attempts to remove the electrolyte from the active materials of the electrodes by leaching with such solvents as pyridine, propylene carbonate saturated with $AlCl_3$, and various alcohols were unsuccessful.

C. Cell Chemistry
(M. F. Roche)

1. Metallographic Study of FeS Electrodes
(A. E. Martin, Z. Tomczuk)

Studies of the phase changes that occur in iron sulfide electrodes are continuing. Laboratory-scale Li/LiCl-KCl/FeS cells that had been cycled repeatedly at 400°C were terminated at various states of charge and a photographic record was made of the positive-electrode phases. In each cell, the positive electrode consisted of 1 A-hr of FeS (1.6 g) within a 5-cm^2 graphite cup having a porous graphite cover.

Figure IV-6 shows the phases present and the electrode morphology at six stages of charge. All photomicrographs are at the same magnification, and the background phase is LiCl-KCl. In the fully discharged electrode, shown on the upper left, the phases present are large grey particles of Li_2S, small white particles of iron (often as inclusions in Li_2S), and a minor amount of KCl crystals that have the same color as the background. On the upper right, the partial conversion to Li_2FeS_2 platelets is shown. The next photomicrograph (middle, left) shows the mixture of Li_2FeS_2 and Fe that results after 50% charge. As charging is continued (middle, right) the J phase, $LiK_6Fe_{24}S_{26}Cl$, becomes the dominant phase; iron is still present to a minor extent. Charging beyond this stage in the presence of an iron current collector may lead to excessive dissolution of the collector. Conservative practice would dictate stopping at conversion of Li_2S and iron to J phase. In the fully charged electrode on the lower left, the only sulfide phase is FeS, which usually appears as fine, porous crystals. In cells operated at high temperatures, larger, more dense FeS crystals are formed. Overcharge (lower, right) results in formation of $Fe_{1-x}S$, that is, the compound contains more sulfur than stoichiometric FeS; dissolution of iron as $FeCl_2$ in the electrolyte also occurs.

2. Wick and Pool Electrodes for Use in Prismatic and Cylindrical Cells
(S. Faist,* L. E. Ross, M. F. Roche)

A study of novel liquid-lithium-electrode structures for use in prismatic and cylindrical cells has been initiated. The purpose of this study is to find electrode structures that circumvent the dewetting problem of conventional liquid-lithium electrodes. If this problem is solved, the liquid-lithium electrode may perform as well as Li-Al solid electrodes. The development of liquid-lithium electrodes is of interest because Li/FeS_x cells have higher cell voltages and much higher theoretical specific energies than $Li-Al/FeS_x$ cells.

The conventional method of retaining liquid lithium in an electrode is to absorb it in a porous metal substrate of high surface area. However, the absorption process is only partly reversible because of the dewetting that occurs after repeated cycling; as a result, the lithium that is not reabsorbed tends to cause short circuits.[3]

---

*Undergraduate Research Participant, Sweet Briar College, Sweet Briar, VA

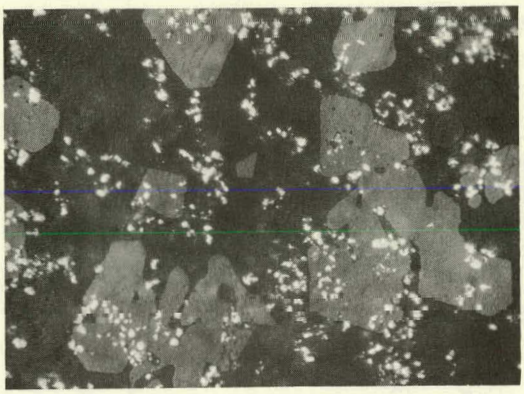

FULLY DISCHARGED. Phases: Li_2S, Fe, KCl.

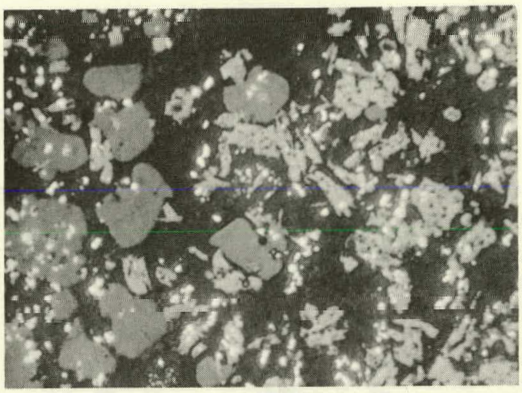

PARTIALLY CHARGED. Phases: Li_2S, Li_2FeS_2, Fe; Li_2S being converted to Li_2FeS_2.

PARTIALLY CHARGED. Phases: Li_2FeS_2, Fe; Li_2FeS_2 dominant.

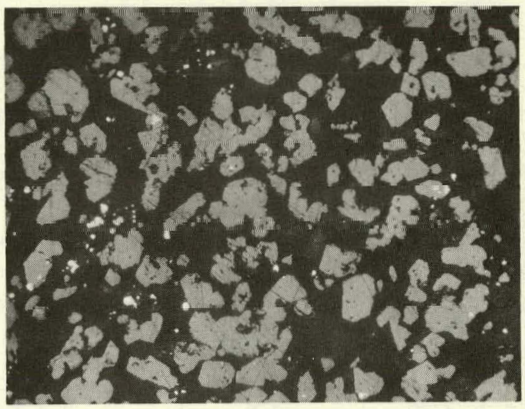

PARTIALLY CHARGED. Phases: J($LiK_6Fe_{24}S_{26}Cl$), Fe; J Phase dominant. (Maximum charge practical with Fe current collector.)

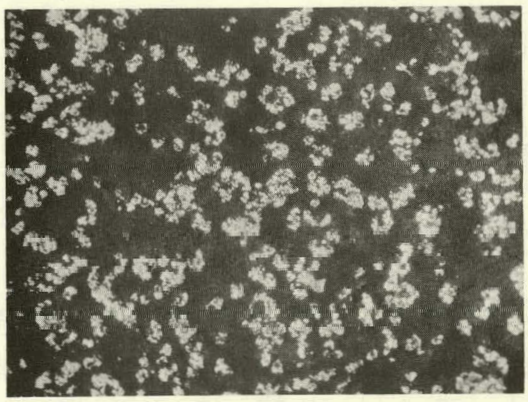

FULLY CHARGED. Phases: FeS only. (Full charge attainable only in the absence of Fe current collector.)

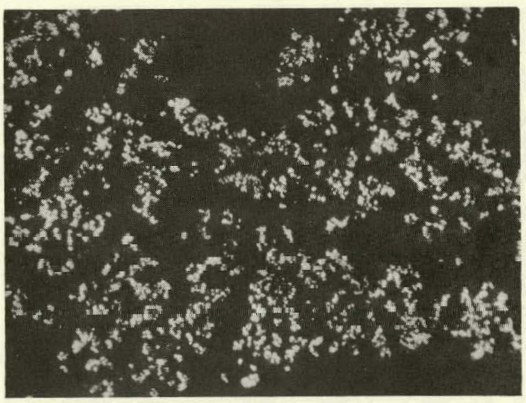

OVERCHARGED. Phases: $Fe_{1-x}S$ only.

Fig. IV-6.

Structure of Positive Electrodes of Li/LiCl-KCl/FeS Cells During Charging (gray background phase is LiCl-KCl eutectic; original magnification 500 X; as-polished; photographically reduced by 38%). ANL Neg. No. 308-76-360

A different approach to liquid-metal-electrode structures is being taken in this study--one that exploits the properties of the liquids more fully. A low-surface-area wick is employed to draw lithium from an isolated pool and down through the electrolyte. Two types of wicks are being considered for this application: a corrugated sheet* with V-shaped grooves to provide a strong capillary force, and fine wires packed within tubing to provide capillary interstices. (The latter type is similar to a heat pipe in its construction.) Three methods by which the pool can be isolated are as follows: (1) floating of the lithium on the electrolyte surface within a retainer ring; (2) retention of the lithium in an inverted cup on the electrolyte surface, with the cup raised slightly to create a partial vacuum that holds the lithium in place; and (3) placement of the lithium in a container separated from the cell so that the lithium is lower than the electrolyte surface. Conventional liquid-metal electrodes combine the lithium-wicking and lithium-storage functions and are more restrictive than the present concept, which permits independent optimization of the wick and storage capabilities.

The first test of a lithium wick-and-pool electrode was conducted in a Li/LiCl-KCl/Al cell. The lithium pool was confined on the electrolyte surface in an open tantalum tube. A corrugated iron sheet (6 vertical channels 0.6 cm deep and 0.15 cm wide) penetrated the pool and extended through the electrolyte to a small aluminum test electrode (capacity, 0.2 A-hr on the basis of formation of LiAl) that was located at a depth of 12 cm. The cell was operated for 16 cycles at 65 mA/cm^2 with a utilization of 75%. The resistances measured with the wick positioned as described above and with the lower end of the wick just contacting the lithium pool were 220 and 365 mΩ, respectively; these measurements demonstrated that the wick was functioning. However, when the wick was removed and examined, four of the channels were filled to a depth of approximately 9 cm, but two had failed to wet completely and were filled to only a 5-cm depth. Lithium/iron sulfide cells that employ the pool-and-wick electrode are being constructed to provide a more stringent test of the concept.

3. Lithium-Silicon Electrodes

(D. R. Vissers, W. R. Frost, M. F. Roche, K. E. Anderson)

Lithium-silicon electrodes were first studied at Atomics International (AI).[4] Studies at ANL[5] were directed toward optimization of electrode capacity as a function of current density. A more detailed examination of the data from the Li-Si/LiCl-KCl/Li cell tests at ANL was undertaken, and other cells were operated to further test the Li-Si electrode in LiF-LiCl-LiBr and in LiCl-KCl electrolytes.

Results of recent studies showed good agreement with AI data on compounds formed in the Li-Si system, and a better understanding has been gained of the problem of irreversible losses of silicon by compound formation with current collector materials. This problem (and a second problem of poor polarization characteristics) need to be solved before silicon can be considered a satisfactory electrode material. The solution will require either incorporation of the silicon in a chemical compound to lower the silicon activity or improvements in the conventional current collectors that will result in lessened silicon attact.

---

*Suggested by J. Eberhart (Cell Chemistry Group).

Figure IV-7 shows that the decline in observed Li-Si plateau lengths is proportional to the square root of time of operation. Data are plotted for two cells. Cell JW-1 employed LiCl-KCl eutectic and operated at 425°C. Cell MR-1 employed 22 mol % LiF-31 mol % LiCl-47 mol % LiBr and operated at 490°C, except for the final discharge, which was at 580°C. The loss in plateau lengths with cycling has been traced to reaction with the nickel current collector and stainless steel electrode housings to form silicides. In the case of the high-temperature cell (MR-1) δ-Ni_2Si was identified by X-ray examination, and metallographic studies showed that 90% of the nickel Retimet current collector had reacted.*

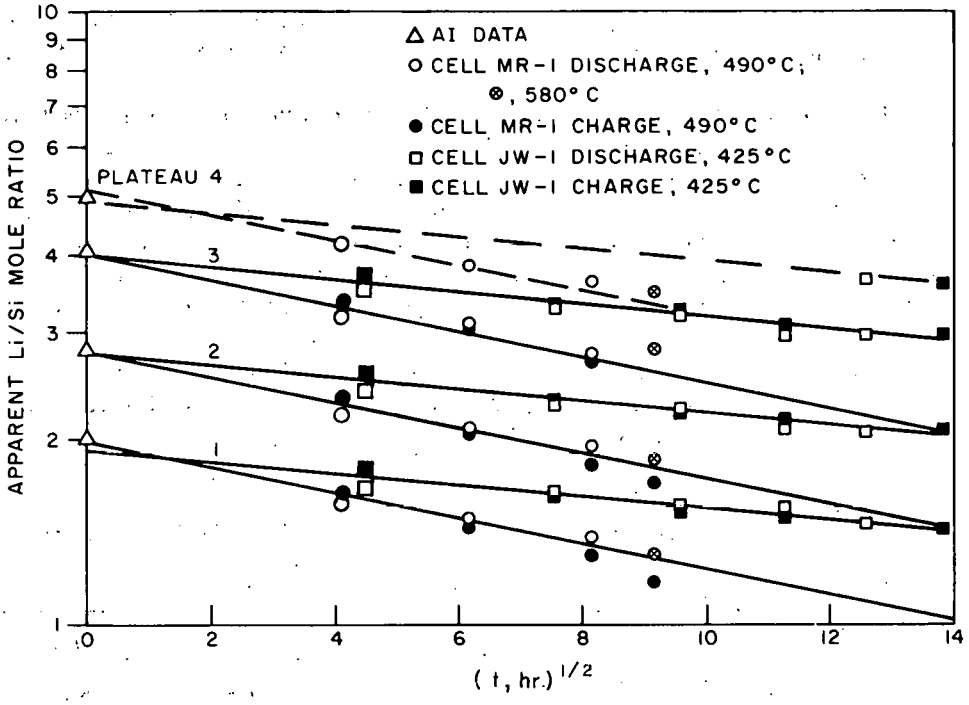

Fig. IV-7.

Decline in Li-Si Plateaus with Cycling Owing to Reaction of Silicon with Housing and Current Collector (AI data from Ref. 4)

The data in Fig. IV-7, which show a dependence of Li/Si ratio on the square root of time, are indicative of a film-formation reaction that is controlled by diffusion. These curves were plotted on the assumption that silicon loss occurred when the silicon activity was high (*i.e.*, on the first plateau, which is a mixture of Li_2Si and Si that has a silicon activity of one). Therefore, the values of t chosen for the plot of the first charge represent the time to charge Si to Li_2Si (the cell was assembled with the electrodes uncharged). The first discharge of the Li-Si compounds would again

*Metallography studies by F. C. Mrazek of the Materials Development Group; X-ray studies by B. S. Tani of the Analytical Chemistry Laboratory, ANL.

lead to silicon loss on the (Li_2Si, Si) plateau, but this would not affect the lengths of the discharge plateaus because lithium is not lost by corrosion. Consequently, the first discharge was plotted at the same time position as the first charge. For later charges, loss of silicon was considered to have taken place during the charge itself and during the preceding (Li_2Si, Si) discharge. Thus, if C1 and D1 were plotted at a time $(t_1)^{1/2}$, C2 and D2 would be plotted at $(3t_1)^{1/2}$, where t_1 is the time for charge or discharge.

Measurements of the plateau lengths at AI were made by starting with a Li-Si alloy that contained excess lithium.[4] Therefore, the plateau lengths during the first discharge would have been unaffected by Si loss. In the AI studies, the compounds formed in the Li-Si system were cited as Li_5Si, $Li_{4.1}Si$, $Li_{2.8}Si$ and Li_2Si. These are plotted as triangles at zero time. Extrapolation of our cell data to zero time is seen to be in good agreement with the AI data.

Plateau emfs were measured on extended open circuit over a wide temperature range in Cells MR-1 and JW-1 and also in Cell MR-2. Cells JW-1 and MR-1 employed Li (3.5 mol % Cu) as a reference and counter electrode, but Cell MR-2 employed a pure lithium reference/counter electrode that, we believe, gave more acceptable results for purposes of thermodynamic calculations. The emf data were within 1 mV of the least-square fit for both the Li(Cu) and Li cells. The equations for the curves are compared in Table IV-3 with those reported by AI. The results for all ANL cells agree within a few millivolts at 400°C, and the equations for Cell MR-2 and for AI data are in fair agreement except for the (Li_2Si, $Li_{2.8}Si$) plateau. The data indicate that all four compounds are stable to at least 580°C.

Table IV-3. Voltages of Plateaus in the Li-Si System

	Emf *vs.* Li		
		This Study	
Plateau	AI[a] (633-713 K)	Cell MR-2 (648-773 K)	Cells JW-1, MR-1[b] (673-853 K)
	Equations		
Si, Li_2Si	430.7-0.1402 T	422.0-0.126 T	416.3-0.120 T
Li_2Si, $Li_{2.8}Si$	332.1-0.0771 T	364.4-0.1182 T	355.4-0.1077 T
$Li_{2.8}Si$, $Li_{4.1}Si$	276.5-0.1761 T	272.9-0.1662 T	257.3-0.1448 T
$Li_{4.1}Si$, Li_5Si	137.7-0.1336 T	126.7-0.1114 T	106.5-0.0854 T
	Corresponding Emfs, mV, at 673 K		
Si, Li_2Si	336	337.1	335.8
Li_2Si, $Li_{2.8}Si$	280	284.8	282.9
$Li_{2.8}Si$, $Li_{4.1}Si$	158	161.0	159.8
$Li_{4.1}Si$, Li_5Si	48	51.7	49.0

[a]Ref. 4.

[b]These cells have lower emfs than Cell MR-2 because Li(3.5 mol % Cu) was used as a reference/counter electrode; Cell MR-2 and AI cells employed pure Li.

D. Alternative Secondary Cells

(M. F. Roche, W. J. Walsh)

The objective of this work is the development of new secondary cells, with emphasis being placed on the use of inexpensive, abundant materials. The experimental work ranges from cyclic voltammetry and preliminary cell tests through construction and operation of engineering-scale cells for the more promising systems. At present the studies are being focused on development of new electrodes for molten-salt cells.

1. Preliminary Tests of New Systems

(Z. Tomczuk, A. E. Martin, C. Sy)

Small cells are being operated to evaluate the suitability of various electrochemical couples for use in secondary cells. These cells employ electrodes with areas of 5 cm^2; the container for the positive-electrode material is a graphite cup with a porous-graphite cover, and the negative electrodes are housed in stainless steel.

The preceding quarterly report (ANL-76-81, p. 53) gave the results of a test of a $LiAl/TiS_2$ cell in LiCl-KCl. In that cell some gassing was observed, and the utilization of TiS_2 (to form $LiTiS_2$) was only 40%. A utilization of 100% has now been obtained in three $Li/LiCl-KCl/TiS_2$ cells operated at 420°C. As in the $LiAl/TiS_2$ cell, the positive-electrode capacity was 0.25 A-hr (1.05 g TiS_2); a detailed metallographic examination and X-ray study* of the discharge products from these electrodes has shown that they consist of interconnected platelets of $LiTiS_2$, in agreement with Whittingham's results for ambient-temperature Li/TiS_2 cells.[6] The performance of the TiS_2 electrode is quite good, as can be seen from the voltage curves in Fig. IV-8, which show that 100% utilization is obtained even at high current density (98 mA/cm^2). The emf of the Li/Li_xTiS_2 couple, which declines from 2.33 V at full charge ($x = 0$) to 1.73 V at $x = 0.8$, is lower than that for the ambient temperature cell[6] (2.45 V at full charge and 2.07 V at $x = 0.8$), but the polarization characteristics in the molten-salt cell are superior.

In the preceding report (ANL-76-81, p. 53), the value given for the emf of a Na/FeS_2 cell operated at 420°C was 1.545 V. The cell had an electrolyte of LiCl-KCl eutectic containing 10 mol % NaCl. It has since been determined that FeS_2 in positive electrode had been converted to Li_2FeS_2, which was never recharged to FeS_2. Moreover, emf measurements on this type of cell showed that the emf on the FeS_2 plateau was 1.98 V and on the Li_2FeS_2 plateau, 1.545 V.

To clarify these results, four additional $Na/LiCl-NaCl-KCl/FeS_2$ cells were operated and terminated at various states of charge; samples were then taken for X-ray* and metallographic studies. Except for indications that NaCl had precipitated during cell operation, the results for the positive electrode were the same as those for FeS_2 in $Li/LiCl-KCl/FeS_2$ cells. Iron and Li_2S were found in the fully discharged cell; Li_2FeS_2 was the phase present at 50% charge; and FeS_2, $Li_4Fe_2S_5$, and FeS were found near full charge. The sodium electrode from one of the cells was also analyzed, and 2 wt % Li was found.

---

* X-ray study conducted by B. S. Tani, Analytical Chemistry Laboratory, ANL.

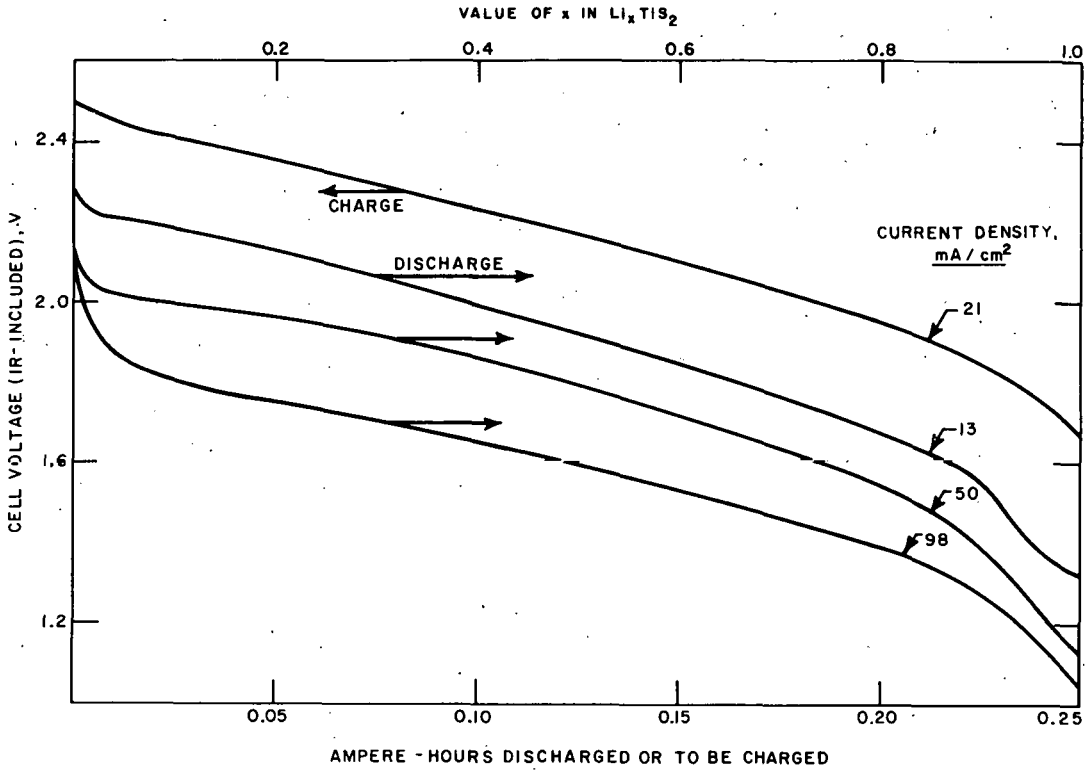

Fig. IV-8. Performance of Li/TiS_2 Cell at 420°C (all discharges preceded by 21 mA/cm^2 charge)

In all these cells, sodium was discharged from the negative electrode, but it remained in the electrolyte as NaCl, and lithium, rather than sodium, was incorporated in the positive electrode. The emfs of these cells are about 50 mV less than those of the corresponding Li/Li_2FeS_2 and Li/FeS_2 cells. Further tests are planned to determine the effect of NaCl additions on the chemistry and performance of FeS and LiAl electrodes.

2. Negative Electrodes of the Second Kind
(S. Von Winbush,* S. J. Preto)

Slow-sweep, cyclic-voltammetry studies of the lithium-aluminum and calcium-aluminum compounds in molten-salt electrolytes were described in the preceding report (ANL-76-81, pp.49-51); in addition, ZrO_2 fabric was found to be electroactive in the presence of calcium ion. This last observation led to the present study of negative electrodes that employ mixtures of reactive metals (or their alloys) with lithium (or calcium) oxides and sulfides. In this type of electrode, called an electrode of the second kind,[7-9] the metal discharges to form an oxide or sulfide precipitate, and lithium (or calcium) ions are released to carry current through the electrolyte. For example, one mole of LiAl may discharge to $LiAlO_2$ in the presence of Li_2O, with the release of four moles of lithium ion. The attractive features of this type of electrode are as follows: 1) the metal can be cycled reversibly

*Research Participant, State University of New York, Old Westbury, NY

without requiring a significant concentration of its ion in the salt, 2) the discharge of the metal is shifted toward strongly anodic potentials because of the low metal-ion concentration in the salt, and 3) the metal can be deposited as a mixture of fine powders rather than dendrites. Note that the positive electrodes of LiAl/LiCl-KCl/iron sulfide cells are, in fact, positive electrodes of the second kind since, in these electrodes, mixtures of Fe and Li_2S are converted to iron sulfides and lithium ions.

The electrodes that were tested by cyclic voltammetry for their ability to operate as negative electrodes of the second kind were mixtures of Al, Mg, or Ti with an excess of lithium or calcium oxides and sulfides. Tests with lithium oxide or sulfide were conducted in LiCl-KCl eutectic at 460°C and, with calcium oxide or sulfide, in LiCl-KCl-$CaCl_2$ (54.5, 14.5, and 31 mol %, respectively) at 500°C. The reference and counter electrodes were LiAl (in LiCl-KCl) and $CaAl_2$ (in LiCl-KCl-$CaCl_2$).

Peak capacities consistent with formation of electrodes of the second kind were found in two cases: 1) mixtures of Al (charged to LiAl) with Li_2O, and 2) mixtures of Mg (charged to LiMg) with Li_2O. Other mixtures underwent simple alloy formation and discharge (for example, formation and discharge of $CaAl_4$ and $CaAl_2$ with calcium ions and aluminum) or produced low-capacity peaks indicative of poor kinetics (for example, all tests with titanium).

In the case of Al (23.8 mg) and excess Li_2O, charged to LiAl and Li_2O, the discharge peaks had emfs of -80 mV (25 mA-hr), zero mV (28 mA-hr, complex) and approximately -200 mV (10 mA-hr) relative to LiAl. At least two Faradays per mole of Al were obtained within the range -300 to +300 mV *vs.* LiAl, and about four Faradays per mole of Al were obtained over a wide anodic range (-300 to +900 mV *vs.* LiAl). The value of four Faradays is equivalent to discharge of LiAl to $LiAlO_2$. With the magnesium electrode (62.5 mg Mg) and excess Li_2O, charged to LiMg and Li_2O, a two-electron peak (132 mA-hr) with an emf of -200 mV *vs.* LiAl and a one-electron peak (58 mA-hr) at approximately 350 mV *vs.* LiAl were observed. For both the (LiAl, Li_2O) and (LiMg, Li_2O) mixtures, the peaks described above occurred during each cycle of the electrode. The data indicate that these alloy-oxide mixtures act as reversible electrodes of the second kind, but it was not possible to determine the electrode compounds or to predict in-cell performance from these voltammetry experiments.

Characterization of the electrode compounds will require metallographic and X-ray analysis. In addition, in-cell tests will be conducted. For the cell tests, a positive electrode based on oxide formation and discharge will be needed. To this end, studies of the Li-Fe-O system have been initiated.

3. Engineering Cell Tests
(W. R. Frost, D. R. Vissers)

An intermediate-scale (∿14 cm dia) $CaMg_2$/FeS cell has been fabricated and is being operated at 480°C. The capacity of the $CaMg_2$ electrode is 60 A-hr and that of the FeS electrode, 90-A-hr; the electrolyte is LiF-LiCl-KCl-$CaCl_2$ (mp, ∿400°C). At present, the cell has been operated through three cycles with an ampere-hour efficiency of ∿100%. In these early cycles, the calcium utilization has ranged from 60% at a 10 mA/cm^2 rate to 28% at a 25 mA/cm^2 rate (current densities based on 93.3 cm^2 active electrode area). On the basis of experience with other cells, the electrical performance of this cell is expected to increase with continued cycling.

V. Li-Si/FeS CELL AND BATTERY DEVELOPMENT--ATOMICS INTERNATIONAL

A cell and battery development program by the Atomics International Division of Rockwell International is directed primarily toward application of the Li-Si/LiCl-KCl/FeS system to stationary energy storage. This program is funded jointly by the Electric Power Research Institute, Atomics International, and Argonne National Laboratory. That portion of the work contracted by Argonne involves the development of iron sulfide electrodes, the long-term testing of cells, the development of ceramic components, the construction and testing of compact, high-energy-density bicells, and the construction and testing of a 1.0-kW-hr demonstration cell.

The work on iron sulfide electrode development currently consists of tests of 25 cm^2 FeS electrodes in compact cells that have volumetric capacities in the range of 0.8-1.0 A-hr/cm^3. In the long-term cell tests, a 150 W-hr demonstration cell has been operated through 1,120 charge-discharge cycles over a period of 11,370 hr, and the test is continuing at the C/4 rate. In the work on ceramic components, attention is being focused on the fabrication of rigid, porous ceramic separators and their testing for compatibility in lithium/electrolyte and lithium-silicon alloy/electrolyte mixtures at 420°C. The cell development effort is concerned mainly with the scale-up of compact cells having volumetric capacities of about 1.0 A-hr/cm^3 in both electrodes. A 1 kW-hr demonstration cell has completed 65 charge-discharge cycles in 1400 hours of operation. The coulombic efficiency has remained in the range of 95-99%. At the C/10 rate, the utilization of active materials is 66%, the specific energy $\sim$80 W-hr/kg, and the energy efficiency 74-77%. At the C/5 rate, the corresponding values are 56% utilization, 54 W-hr/kg specific energy, and 71% energy efficiency.

REFERENCES

1. D. R. Vissers and K. E. Anderson, *The Characterization of Porous Li-Al Alloys*, Proc. Symp. and Workshop on Advanced Battery Research and Design, ANL-76-8, p. B-176 (1976).

2. H. Shimotake and L. G. Bartholme, *Development of Uncharged Li-Al/FeS Cells*, Proc. Symp. and Workshop on Advanced Battery Research and Design, Argonne National Laboratory, ANL-76-8, pp. B-210 - B-218 (1976).

3. See, for example, U. S. Patent No. 3,881, 951, *Lithium Electrode and Method of Producing the Same*, L. R. McCoy (assigned to Atomics International) 1975.

4. San-Cheng Lai, J. Electrochem. Soc. *123*, 1196 (1976).

5. W. R. Frost *et al.*, Paper No. 20, Extended Abstracts, Electrochem. Soc. Mtg., Washington, D. C., May 2-7, 1976; also ANL-76-35, pp. 50-52 (April 1976).

6. M. S. Whittingham, J. Electrochem. Soc. *123*, 315 (1976).

7. S. Glasstone, *Introduction of Electrochemistry*, 8th ed., D. van Nostrand Co., New York, p. 184 (1959).

8. K. J. Vetter, *Electrochemical Kinetics*, Academic Press, New York, pp. 23, 32 (1967).

9. G. Kortum and J. O'M. Bockris, *Textbook of Electrochemistry*, Vol. 1, Elsevier Press Co., New York, p. 241 (1951).

APPENDIX.

SUMMARY OF LARGE-SCALE CELL TESTS

APPENDIX. Summary of Large-Scale Cell Tests

Cell or Battery No.	Type of Cell	Operating Characteristics: Capacity, A-hr: Theor.	Operating Characteristics: Capacity, A-hr: Max.[a] at Indicated Rates	Operating Characteristics: Rates, hr: Disch.	Operating Characteristics: Rates, hr: Charge	Initial Eff.,[b] %: A-hr	Initial Eff.,[b] %: W-hr	Life Characteristics: Hours[c]	Life Characteristics: Cycles[c]	Life Characteristics: % Decline in: Capacity[d]	Life Characteristics: % Decline in: A-hr Eff.	Remarks
2B4	Li-Al/ FeS_2-CoS_2	149	104 99 97.5 69.5	8.0 6.2 5.0 2.0	8.0 7.6 7.5 5.3	99+	80	1697	130	~40	0.3	Eagle-Picher thick electrodes. Operation terminated because of decline in capacity.
2A5	Li-Al/ FeS_2-CoS_2	69	55.6	5.6	5.6	99+	83	>910	>72	7	3	Eagle-Picher thin electrodes. Max. specific energy, 65.8 W-hr/kg (5.6-hr rate); presently, 52 W-hr/kg (5.3-hr rate).
2B5	Li-Al/ FeS_2-CoS_2	149	114.7	8.8	8.8	99+ (8.8)	80 (8.8)	>1050	>55	16	None	Eagle-Picher thick electrodes. Higher charge cutoff (2.1 *vs.* 2.0 V for 2B4). Capacity is 15% higher than that of 2B4.
2B8	Li-Al/ FeS_2-CoS_2	149	118 117	11.8 9.0	11.8 9.0	99 (9)	82 (9)	> 264	>13	2	None	Start-up and operation with cell blanketed in Kaowool insulation, exposed to air.
B6-S	Li-Al/ FeS-Cu_2S	149	76	7.6	7.6	99	83	192	14	-	-	Eagle-Picher thick electrode Cells 1B4, 1B5, B6. Terminated because of declining capacity and A-hr eff. Cell 1B5 removed for post-test exam. Operation of 1B4 and 1B6 continued in B7-S.
B7-S	Li-Al FeS-Cu_2S	149	100 77 57 35	10 5.1 2.8 1.4	8.5 6.2 4.1 3.5	99	80	>2016	>92	None	None	Eagle-Picher thick electrode cells in series. Total life of 1B4 is 3200 hr, 156 cycles; 1B6, 2560 hr, 129 cycles. Being operated with bulk charge + 4 hr equalization.
B8-P	Li-Al/ FeS_2-CoS_2	149	113 90	5.6	5.6	99	83	480	30	-	-	Eagle-Picher thin electrode Cells 2A3, 2A4 in parallel. Startup/conditioning test. Terminated after performance testing. Cells used in B8-S.
B8-S	Li-Al/ FeS_2-CoS_2	69	50 50 44 24	9.9 5.0 2.2 1.2	10 4.5 6.2 4.9	98	78	>1080	>105	19	None	Eagle-Picher thin electrode cells (2A3 and 2A4) in series. Total life of each cell is 1560 hr, 135 cycles. Being operated with bulk charge only.

(contd)

APPENDIX. (contd)

Cell or Battery No.	Type of Cell	Operating Characteristics: Capacity, A-hr: Theor.	Operating Characteristics: Capacity, A-hr: Max.[a] at Indicated Rates	Operating Characteristics: Rates, hr: Disch.	Operating Characteristics: Rates, hr: Charge	Initial Eff.,[b] %: A-hr	Initial Eff.,[b] %: W-hr	Life Characteristics: Hours[c]	Life Characteristics: Cycles[c]	Life Characteristics: % Decline in: Capacity[d]	Life Characteristics: % Decline in: A-hr Eff.	Remarks
R-6	Li-Al/ $FeS-Cu_2S$	73	47	5	9	96	86	6678	635	70	16	Assembled uncharged; 10 mol % Cu_2S in FeS. Capacity declining, terminated for examination.
R-8	Li-Al/ FeS_2-CoS	85	72	10	10	99	85	3300	438	59	58	Assembled uncharged; hot-pressed positive electrode with Li_2S from Eagle-Picher; one-piece Mo current collector/lead. Terminated (short circuit).
R-12	Li-Al/ $FeS-Cu_2S$	105	58	6	8	89	69	3210	173	20	60	Assembled uncharged; 20 mol % Cu_2S in FeS; also, CaC_2 added to positive electrode. Terminated voluntarily.
R-13	Li-Al/ $FeS-Cu_2S$	50	34	5	5	78	64	>2424	>303	35	8	Assembled uncharged; 20 mol % Cu_2S in FeS; electrolyte, 10 wt % $CaCl_2$ in LiCl-KCl eutectic.
R-14	Li-Al/ FeS	106	80	5	10	80	67	1294	80	20	20	Assembled uncharged. High-pressure pressing of positive plaque for low contact resistance. Terminated for examination.
R-15	Li-Al/ FeS_2-CoS	168	109	5	7	98	57	>650	>42	9	None	Assembled uncharged; FeS_2-CoS in honeycomb structure; pressed Al wire negative.
R-18	Li-Al/ FeS	120	65	5	7	97	80	>630	>62	8	8	Assembled uncharged; FeS, no additives. Woven Al plaques with Cu strands in negative electrodes.
R-19	Li-Si/ $FeS-Cu_2S$	120	81	16	16	95	80	>150	>10	8	10	Assembled charged; $FeS-Cu_2S$ positive; negative, Li_4Si powder in compartmentalized structure.
A-1	Li-Al/ FeS_2-CoS	426	242	8	13	88	68	1075	31	30	58	Test of multiple-electrode cell assembled uncharged. 321 W-hr at 8-hr rate. Cell weight, ~3 kg. Terminated; short circuit.

(contd)

APPENDIX . (contd)

Cell or Battery No.	Type of Cell	Operating Characteristics: Capacity, A-hr: Theor.	Operating Characteristics: Capacity, A-hr: Max.[a] at Indicated Rates	Operating Characteristics: Rates, hr: Disch.	Operating Characteristics: Rates, hr: Charge	Initial Eff.,[b] %: A-hr	Initial Eff.,[b] %: W-hr	Life Characteristics: Hours[c]	Life Characteristics: Cycles[c]	Life Characteristics: % Decline in: Capacity[d]	Life Characteristics: % Decline in: A-hr Eff.	Remarks
KK-4	Li-Al/ FeS_2-CoS_2	90	87	5	5	99	79	>4600	>280	50	6	Assembled charged; carbon-bonded FeS_2-CoS_2 and hot-pressed Li-Al. Cell resistance 5.8 mΩ, with Mo current collector.
KK-5	Li-Al/ FeS-$CuFeS_2$	120	93	5	10	99	85	>3100	>170	1	None	Assembled uncharged; carbon-bonded Li_2S + Fe + Cu and Al wire plaque + Li-Al hot-pressed electrode. Terminated for electrode exam, then restarted. Cell retains high utilization and 3.8 mΩ resistance.
KK-6	Li-Al/ FeS_2-CoS_2	150	94	5	10	99	72	>2500	>155	None	None	Assembled uncharged; carbon-bonded Li_2S + Fe + CoS_2 and 32 at. % Li-Al solid plate electrodes. Cycled at 10-hr rate, >75 W-hr/kg.
SS-1	Li-Al/ FeS-Cu_2S	650	432	5	10	100	85	>750	>40	4	None	Assembled charged; carbon-bonded FeS-Cu_2S and Li-Al in Fe Retimet. Designed for utility application. Operating well in start-up cycles.
CB-1	Li-Al/ $CuFeS_2$	147	67	5.3	5.5	93	63	>5350	>365	None	4	Charged, carbon-bonded $CuFeS_2$ electrode; hot-pressed Li-Al negative electrode. Open cell in sealed furnace well. Performance stable.
MP-2	Li-Al/ FeS_2-CoS_2	119	61	5.0	5.0	96	77	>1925	>163	15	4	Test of multiplate, charged cell with two carbon-bonded positive electrodes and four negative electrodes of Li-Al in iron Retimet. Being operated with constant-voltage charging.
FM-1	Li-Al-In/ FeS-Cu_2S	75	46	6	6	99	85	>325	>30	None	None	Charged Eagle-Picher FeS-Cu_2S positive electrode, Li-Al-4 wt % In negative electrode. Performance improving during early cycling.

[a] Based on at least five cycles.
[b] Based on at least 10 cycles at the 5-hr rate.
[c] The "greater than" symbols denote continuing operation.
[d] Percent decline from max. capacity at 5-hr rate, except where noted.

Distribution for ANL-76-98

Internal:

M. V. Nevitt
R. V. Laney
P. R. Fields
S. A. Davis
B. R. T. Frost
G. T. Garvey
D. C. Price
K. E. Anderson
J. D. Arntzen
J. Barghusen
L. Bartholme
J. E. Battles
E. C. Berrill
C. A. Boquist
L. Burris
F. A. Cafasso
A. A. Chilenskas
T. Cooper
P. Cunningham
D. Day
J. Dorsey
J. G. Eberhart
R. Elliott
W. R. Frost
E. C. Gay
F. Hornstra
A. A. Jonke
R. W. Kessie
G. M. Kesser (2)
V. M. Kolba
W. Kremsner
M. L. Kyle
W. W. Lark
S. Lawroski
C. A. Luartes
R. F. Malecha
A. E. Martin
F. J. Martino
C. A. Melendres
A. Melton
W. E. Miller
F. Mrazek
K. M. Myles
T. Olszanski
P. A. Nelson (100)
E. G. Pewitt
E. R. Proud
S. Preto
G. Redding
M. F. Roche
L. E. Ross
J. Royal
W. W. Schertz
J. L. Settle
H. Shimotake
J. A. Smaga
R. K. Steunenberg
C. A. Swoboda
A. D. Tevebaugh
W. D. Tuohig
Z. Tomczuk
D. R. Vissers
S. Vogler
W. J. Walsh
D. S. Webster
I. O. Winsch
S. E. Wood
N. P. Yao
S. A. Zivi
P. Eshman
J. E. A. Graae
J. L. Hamilton
J. Mathers
G. J. Bernstein
K. G. Carroll
P. A. Eident
T. D. Kaun
J. E. Kincinas
K. Kinoshita
Z. Nagy
K. A. Reed
M. A. Slawecki
C. Sy
J. Williams
A. B. Krisciunas
ANL Contract Copy
ANL Libraries (5)
TIS Files (6)

External:

ERDA-TIC, for distribution per UC-94c (180)
Chief, Chicago Patent Group
V. Hummel, ERDA-CH
President, Argonne Universities Association
Chemical Engineering Division Review Committee:
R. C. Axtmann, Princeton Univ.
R. E. Balzhiser, Electric Power Research Institute
J. T. Banchero, Univ. Notre Dame
D. L. Douglas, Gould Inc.
P. W. Gilles, Univ. Kansas
R. I. Newman, Allied-General Nuclear Services
G. M. Rosenblatt, Pennsylvania State Univ.
J. G. Ahlen, Illinois Legislative Council, Springfield
J. N. Anand, Dow Chemical Co., Walnut Creek, Calif.
F. Anson, California Inst. Technology
P. Auh, Brookhaven National Laboratory
B. S. Baker, Energy Research Corp.

H. Balzan, Tennessee Valley Authority
K. F. Barber, Div. Transportation Energy Conservation, USERDA
H. J. Barger, Jr., U. S. Army MERDC, Fort Belvoir
T. R. Beck, Electrochemical Technology Corp., Seattle
J. A. Belding, Div. Conservation Research & Technology, USERDA
M. Benedict, Massachusetts Institute of Technology
D. N. Bennion, Univ. California, Los Angeles
J. Birk, Electric Power Research Inst.
J. Braunstein, Oak Ridge National Laboratory
M. Breiter, GE Research & Development Center
J. O. Brittain, Northwestern U.
R. Brodd, Parma Technical Center, Union Carbide Corp.
J. J. Brogan, Div. Transportation Energy Conservation, USERDA
E. Brooman, Battelle Memorial Institute, Columbus
D. M. Bush, Sandia Laboratories
E. Buzzelli, Westinghouse Electric Corp., Pittsburgh
E. J. Cairns, General Motors Research Lab., Warren, Mich.
E. Carr, Eagle-Picher Industries, Joplin
P. Carr, Energy Development Associates, Madison Heights, Mich.
Chloride Systems (U. S. A.) Inc., North Haven, Conn.
C. Christenson, Gould Inc.
M. Cohen, Univ. of Chicago
A. R. Cook, Int'l Lead Zinc Research Organization, Inc., New York City
D. R. Craig, Hooker Chemical Corp.
G. Cramer, Southern California Edison, Rosemead
W. Dippold, Div. Transportation Energy Conservation, USERDA
J. Dunning, General Motors Research Lab., Warren, Mich.
P. Eggers, Battelle Memorial Institute, Columbus
R. P. Epple, Div. Physical Research, USERDA
J. H. B. George, Arthur D. Little, Inc.
J. Giner, Tyco Labs., Inc., Waltham, Mass.
C. Goddard, Div. Conservation Research and Technology, USERDA
G. Goodman, Globe-Union, Inc., Milwaukee
H. Grady, Foote Mineral Co., Exton, Pa.
S. Gratch, Birmingham, Mich.
D. Gregory, Institute of Gas Technology, Chicago
N. Gupta, Ford Motor Co.
N. Hackerman, Rice U.
G. Hagey, Div. of Energy Storage Systems, USERDA
R. Hamilton, Carborundum Co., Niagara Falls
W. Hassenzahl, Los Alamos Scientific Laboratory
L. A. Heredy, Atomics International
B. Higgins, Eagle-Picher Industries, Joplin
R. Hudson, Eagle-Picher Industries, Joplin
J. R. Huff, U. S. Army Mobility Equipment R&D Center, Fort Belvoir
R. A. Huggins, Stanford U.
R. A. Huse, Public Service Electric & Gas Co., Newark, N. J.
S. D. James, U. S. Naval Surface Weapons Center (3)
M. A. Jansen, Allegheny Power Service Corp. Greensburgh, Pa.
G. Janz, Rensselaer Polytechnic Inst.
H. Jensen, C&D Batteries, Plymouth Meeting, Pa.
F. Kalhammer, Electric Power Research Institute
K. Kinsman, Ford Motor Co.
R. Kirk, Div. Conservation Research & Technology, USERDA
K. W. Klunder, Div. of Energy Storage Systems, USERDA

J. Lagowski, Detroit Edison Utility Co.
J. J. Lander, Air Force Aero Propulsion Lab., Wright-Patterson AFB
A. Landgrebe, Div. of Energy Storage Systems, USERDA (6)
C. E. Larson, Bethesda, Md.
S. H. Law, Northeast Utilities, Hartford, Conn.
H. Leribaux, Texas A&M U.
D. Linden, U. S. Army Electronics Command, Fort Monmouth, N. J.
R. Llewellyn, Indiana State U.
P. S. Lykoudis, Purdue Univ.
J. McKeown, Office of Program Administration, USERDA
C. McMurty, Carborundum Co., Niagara Falls
R. McRae, ILC Technology, Sunnyvale, Calif.
D. Meighan, C. & D. Batteries, Plymouth Meeting, Pa.
R. Minck, Ford Motor Co.
F. Moore, Div. of Energy Storage Systems, USERDA
G. Murray, Detroit Edison Utility Co.
E. Nicholson, Esso Research & Engineering Corporate Res. Lab., Linden, N. J.
C. Pax, Div. Transportation Energy Conservation, USERDA
G. F. Pezdirtz, Div. of Energy Storage Systems, USERDA
R. Rightmire, Standard Oil of Ohio, Cleveland
R. Rizzo, Globe-Union Inc., Milwaukee
N. Rosenberg, Transportation Systems Center, Cambridge, Mass.
N. W. Rosenblatt, E. I. duPont de Nemours & Co., Wilmington
R. Rubischko, Gould Inc.
A. Salkind, ESB Inc., Yardley, Pa.
G. Scharbach, American Motors General Corp., Wayne, Mich.
T. Schneider, Public Service Electric & Gas Co., Newark, N. J.
R. I. Schoen, National Science Foundation
J. R. Schorr, Battelle Memorial Institute, Columbus
D. R. Schramm, Public Service Electric & Gas Co., Newark, N. J.
H. J. Schwartz, NASA Lewis Research Center
J. R. Selman, Illinois Institute of Technology
A. I. Snow, Atlantic Richfield Co., Harvey, Ill.
S. Srinivasan, Brookhaven National Laboratory
D. Stakem, Catalyst Research Corp., Baltimore
E. Steeve, Commonwealth Edison Co., Chicago
R. H. Strange II, National Science Foundation
R. L. Strombotne, U. S. Dept. Transportation, Washington
S. Sudar, Atomics International
R. H. Swoyer, Pennsylvania Power and Light Co., Allentown
F. Tepper, Catalyst Research Corp., Baltimore
L. Thaller, NASA Lewis Research Center
G. M. Thur, Div. Transportation Energy Conservation, USERDA
C. W. Tobias, U. California, Berkeley
L. Topper, National Science Foundation
J. Vanderryn, Office of Intern. R&D Programs, USERDA
J. V. Vinciguerra, Eagle-Picher Industries, Joplin
R. D. Walker, Jr., U. Florida
C. O. Wanvig, Jr., Globe Union, Inc., Milwaukee
S. A. Weiner, Ford Motor Co.
J. Werth, ESB Inc., Yardley, Pa.
C. Wienlein, Globe-Union Inc., Milwaukee
F. Will, General Electric R&D Center, Schenectady
J. Withrow, Chrysler Corp., Detroit
W. L. Wonell, U. of California, Berkeley

S. Wood, La Grange Park, Ill.
T. Wydeven, NASA Ames Research Center
O. Zimmerman, Portland General Electric Co., Portland, Ore.
M. Zlotnick, Div. Conservation Research and Technology, USERDA
Chloride Technical Limited, Manchester, England
E. Aiello, U. of Chicago
W. J. Argersinger, Jr., U. of Kansas
J. T. Banchero, U. of Notre Dame
K. J. Bell, Oklahoma State U.
R. Blanco, Oak Ridge Nat. Lab.
C. F. Bonilla, Columbia U.
W. Brandt, U. of Wisconsin-Milwaukee
A. E. Dukler, U. of Houston
W. J. Frea, Michigan Tech. U.
C. D. Harrington, Douglas United Nuclear, Inc.
J. E. Linehan, Marquette U.
Maine Univ., Prof. in charge of Chem. Engr. Lib.
Marquette U., Dept. of Chemistry
Michigan Tech. U., Library
G. Murphy, Iowa State U.
E. A. Peretti, U. of Notre Dame
G. W. Preckshot, Engr. U. of Missouri
H. Rosson, U. of Kansas
C. Sanathanan, U. of Illinois-Chicago Circle
A. Sesonske, Purdue U.
USERDA, Director, Div. of Safeguards and Security
B. W. Wilkinson, Michigan State U.
Comision Nacional de Energia Atomica, Library, Argentina
J. A. Sabato, Com. Nac. de Energia Atomica, Buenos Aires, Argentina
C. H. Cheng, Nat'l Tsing Hua Univ., China
National Radiological Protection Board, Library, Harwell, England
L. Kemmerich, Ges. für Kernforschung, Karlsruhe, Germany
F. Weigel, Inst. für Anorganische Chemie der U. Munich, Germany
N. Saratchandran, Bhabha Atomic Research Centre, Bombay, India
K. Fujimiya, U. of Tokyo, Japan
Japan Atomic Energy Research Inst., Tokai-mura, Japan
K. Matsuda, Inst. of Physical & Chemical Res., Yamato-machi, Japan
Sang-Soo Lee, Korea Advanced Institute of Science, Korea
Korean Atomic Energy Research Institute, Korea
Ragnar Nordberg, Sahlgren's Hospital, Göteborg, Sweden